

# Lawrence Berkeley National Laboratory

## Recent Work

### Title

EXPERIMENTAL TECHNIQUES FOR GROWING UNIDIRECTIONALLY SOLIDIFIED ORIENTED EUTECTICS

### Permalink

<https://escholarship.org/uc/item/4km2p3pw>

### Author

Salmon, Louis Jean.

### Publication Date

1973-06-01

EXPERIMENTAL TECHNIQUES FOR GROWING UNIDIRECTIONALLY  
SOLIDIFIED ORIENTED EUTECTICS

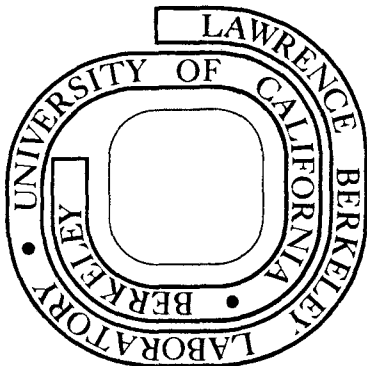
Louis Jean Salmon  
(M.S. thesis)

June 1973

Prepared for the U.S. Atomic Energy Commission  
under Contract W-7405-ENG-48

**For Reference**

Not to be taken from this room



## **DISCLAIMER**

This document was prepared as an account of work sponsored by the United States Government. While this document is believed to contain correct information, neither the United States Government nor any agency thereof, nor the Regents of the University of California, nor any of their employees, makes any warranty, express or implied, or assumes any legal responsibility for the accuracy, completeness, or usefulness of any information, apparatus, product, or process disclosed, or represents that its use would not infringe privately owned rights. Reference herein to any specific commercial product, process, or service by its trade name, trademark, manufacturer, or otherwise, does not necessarily constitute or imply its endorsement, recommendation, or favoring by the United States Government or any agency thereof, or the Regents of the University of California. The views and opinions of authors expressed herein do not necessarily state or reflect those of the United States Government or any agency thereof or the Regents of the University of California.

TABLE OF CONTENTS

ABSTRACT

I. FACTORS WHICH HAVE TO BE CONSIDERED FOR GROWING THE ALIGNED MICROSTRUCTURES . . . . .	1
1. Solidification Characteristics of the Materials . . . . .	1
1.1 Classification of Single Phase Materials . . . . .	1
1.2 Classification of Binary Eutectics . . . . .	1
1.3 Structures Obtained in the Different Groups . . . . .	1
1.4 Modification of Hunt and Jackson Theory . . . . .	2
1.5 Eutectic Temperatures and Compositions . . . . .	3
1.6 Type of Structure as Forecast from the Volume Fraction of Both Phases and the Interfacial Energy . . . . .	3
1.7 Ternary Alloys . . . . .	4
2. Control of Eutectic Microstructure . . . . .	5
2.1 Nucleation and Growth . . . . .	5
2.2 Short-Range Cooperative Growth . . . . .	6
2.3 Discussion of the Freezing Variables . . . . .	7
2.4 Program of Experiments . . . . .	11
3. Purity Requirements for the Materials . . . . .	13
3.1 Commercial Materials . . . . .	13
3.2 Contamination . . . . .	15
4. Temperature Requirements . . . . .	15
4.1 Temperature Setting of the Furnace . . . . .	15
4.2 Temperature Stability . . . . .	15
4.3 Temperature Controller . . . . .	16
4.4 Choice of Thermocouples . . . . .	18

5. Furnaces . . . . .	22
5.1 Similarity with case of single phase materials . . . . .	22
5.2 Eutectics with Melting Points less than 1100°C . . . . .	22
5.3 Simple Physical Arrangements . . . . .	23
5.4 High Melting Points Eutectics . . . . .	23
6. Thermal Gradient Requirement . . . . .	24
6.1 Cases of Small and Large Gradients . . . . .	24
6.2 Temperature Profile of the Furnace . . . . .	24
6.3 Thermal Gradients used in Bridgman-Stockbarger Growth . . . . .	25
6.4 Horizontal Method . . . . .	25
6.5 High Temperature Growth . . . . .	26
7. Molds . . . . .	26
7.1 Mold Materials . . . . .	26
7.2 Shape of the Crucible . . . . .	28
7.3 Size of the Crucible . . . . .	28
7.4 Preparation of Charge . . . . .	29
7.5 Lifetimes of Crucibles . . . . .	29
7.6 Thermal Convection in Horizontal Boats . . . . .	30
7.7 Seeding . . . . .	30
8. Atmosphere Requirement . . . . .	30
8.1 Possibilities . . . . .	30
8.2 Vacuum System . . . . .	30
8.3 Neutral Atmosphere . . . . .	31
9. Rate Requirement . . . . .	32
9.1 Range of Growth Rates . . . . .	32
9.2 Adjustment of the Speed . . . . .	32

9.3	Typical Transmission for an Horizontal Furnace . .	32
9.4	Vertical Design . . . . .	33
II.	EVALUATION OF EUTECTIC MICROSTRUCTURES . . . . .	35
1.	Preparation of Sample. . . . .	35
2.	Characterization of the Material . . . . .	36
2.1	Metallographic Techniques for Optical Microscope . . . . .	36
2.2	X-Ray Techniques . . . . .	41
2.3	Electron Beam Microprobe . . . . .	43
2.4	Transmission Electron Microscope (TEM) . . . . .	44
2.5	Scanning Electron Microscope (SEM) . . . . .	45
2.6	Summary of Methods for Characterization of Oriented Eutectics . . . . .	46
3.	Recent Bibliography about Morphology and Phase Orientations of Oriented Eutectics . . . . .	53
	Acknowledgments . . . . .	55
	References . . . . .	56
	Figures . . . . .	61
	Microphotographs . . . . .	72

EXPERIMENTAL TECHNIQUES FOR GROWING UNIDIRECTIONALLY  
SOLIDIFIED ORIENTED EUTECTICS

Louis Jean Salmon\*

Inorganic Materials Research Division, Lawrence Berkeley Laboratory  
and Department of Materials Science and Engineering, College of Engineering;  
University of California, Berkeley, California

ABSTRACT

The first part of this paper points out the relevant factors for growing aligned eutectics and describes the experimental techniques. The second part presents a review of the methods used for evaluation of the resulting microstructures.

---

\*

Report for the Plan II M. S. Degree given by U. C.  
Department of Engineering

# I. FACTORS WHICH HAVE TO BE CONSIDERED FOR GROWING THE ALIGNED MICROSTRUCTURES

## 1. Solidification Characteristics of the Material

### 1.1 Classification of single phase materials

Experimental observations show that there are two groups of single phase materials, those that grow as faceted crystals and those that do not. A thermodynamic reasoning by Jackson showed that the type of growth depends on the entropy of melting.<sup>(1)(2)</sup> He defined a factor  $\alpha = \xi(\Delta S_F/R)$  where  $\Delta S_F/R$  is the entropy of melting in dimensionless units and  $\xi$  is a crystallographic factor which is less than and almost one.

Most non-metals have an  $\alpha$  greater than 2 and grow with crystalline facets while most metals have an  $\alpha$  less than 2 and grow almost isotropically with no facets.

### 1.2 Classification of binary eutectics

Similarly, Hunt and Jackson<sup>(3)</sup> proposed a classification of binary eutectics based on the entropies of melting of the two eutectic phases. They consider three groups of eutectics. In the first group both phases have low entropies of melting. In the second group one phase has a high and the other has a low entropy of melting. In the third group, both phases have high entropies of melting.

### 1.3 Structures obtained in the different groups

Experimental observations and suitable transparent analogs of the metallic systems showed that the structures obtained are different for the three groups. Eutectics of the first group have lamellar or rod-like structures. Dendrites of either phase may be formed if the alloy is rich in the relevant component. Examples of such systems are Pb-Sn,



Sn-Cd, Pb-Cd, Sn-Zn, Al-Zn. Eutectics of the second group give irregular or complex regular structures. If the alloy is rich in the low entropy of melting, phase dendrites are formed; if it is rich in the high entropy of melting phase, faceted crystals are obtained. Sometimes these crystals are called hoppers or pseudodendrites. Al-Si, Zn-Mg<sub>2</sub>Zn<sub>11</sub>, Pb-Bi, Sn-B are examples of this second group systems. Third group eutectics grow with a faceted solid liquid interface for each phase. Systems of the third group are found between some intermetallics and semiconductors or semimetals such as silicon, germanium, bismuth, rather than with metals.

#### 1.4 Modification of Hunt and Jackson theory

Kerr and Winegard<sup>(4)</sup> report that the BiZn eutectic appears to be lamellar contrary to the Hunt and Jackson theory.<sup>(1,2,3)</sup> One reason for failure of the classification is that the Jackson analysis considers only pure materials. On the other hand, in some eutectic systems which have a large solubility the eutectic temperature can be considerably below the melting point of pure material. Then, use of the entropy of fusion for the pure phase rather than for the solid solution is questionable at the eutectic temperature. Kerr and Winegard calculate  $\Delta F_S$ , the change in surface free energy of an atomically flat interface for a solid solution  $\alpha$  when  $N_A$ , atoms A, and  $N_B$ , atoms B, are added to it and they compute what they call relative free energy,  $\Delta F_S / NKT_E$ , where  $T_E$  is the eutectic temperature and N the total possible number of sites on the added plane, as a function of the occupied fraction of surface sites for both phases. Results found from the study of five eutectics; Bi-Sn, Bi-Pb, Bi-Tl, Bi-Ag and Bi-Zn show that if the resulting relative

free energies are close together, the eutectic is lamellar (Bi-Ag, Bi-Zn) but if they are widely separated, the eutectic is regular (Bi-Sn, Bi-Pb, Bi-Tl).

#### 1.5 Eutectic temperatures and compositions

A large number of binary eutectic temperatures and compositions can be obtained from "Constitution of Binary Alloy" by M. Hansen and K. Anderko. (5) In some not so well known cases, eutectics compositions have to be determined or re-determined. Selected values of thermodynamic properties of metals and alloys may be found from Ref. 6.

#### 1.6 Type of structure as forecast from the volume fraction of both phases and the interfacial energy

The eutectic will freeze in that form which has the lowest inter-phase surface energy for any given separation  $\lambda$ . It is useful to compare the lamellar and fibrous arrangements from that viewpoint. (7) If the further assumption is made that the possible forms have equal ratios  $\alpha/\beta$  surface energies per unit area, it is found that at low volume fractions up to 0.28 any eutectic might be expected to freeze with a fibrous habit while for higher volume fractions a lamellar arrangement would be more probable. In a fibrous structure, the fibres will be of that phase having the smaller volume fraction. However, lamellar eutectics have characteristic orientation relations between the adjacent lattices and of the faces between them. For some orientations of the planar lamellar surfaces which have a lower energy than others, the corresponding arrangements are stabilized. Cooksey, et al., (7) termed these interfaces coincident. If a lamellar surface had a surface energy per unit area of one half that of the less coincident fibre interface, the calculation shows that the lamellar form would then be stable down to a volume

fraction of 0.08. See Fig. 1. Examples of eutectic systems are given in Table I.

Table I. Examples of eutectic systems

System	Composition (at.%)	Temperature (°C)	Composition range	Volume fraction
Al-Ag <sub>2</sub> Al	62.6 Al	566	42-76 Al	0.47 Al
Al-CuAl <sub>2</sub>	82.7 Al	548	68-97.5 Al	0.40 CuAl <sub>2</sub>
Al-Zn	88.7 Zn	382	66.5-97.6 Zn	0.26 Al
Al-Al <sub>3</sub> Ni	2.7 Ni	640	0-25 Ni	0.07 Al <sub>3</sub> Ni
Ag-Cu	40.0 Cu	779	14-95 Cu	0.26 Cu
LiF-NaF	38.0 NaF	640	0-100	0.40 NaF
NaF-NaCl	35.0 NaF	676	0-100	0.22 NaF

Fiber morphology is characteristic of many alloy systems such as Al-Al<sub>3</sub>Ni, Fe-FeS, Ni-Al-Cr, Cu-Cr, MnSb-Sb, InSb-Sb, InSb-NiSb, NaF-NaCl, Fe-Fe<sub>2</sub>Ti, Fe-FeBe<sub>2</sub>, Fe-Fe<sub>2</sub>Zr, FeCo-FeCoB, Co-Au. Lamellar structure is characteristic of eutectics such as Al-CuAl<sub>2</sub>, Cd-Sn, Al-Zn, Co-CoBe, Bi<sub>2</sub>Te<sub>3</sub>-Te, SnSe-SnSe<sub>2</sub>, LiF-NaF, CaF<sub>2</sub>-LiF. Some have approximately equal volume fractions such as Al-Al<sub>2</sub>Cu. Others such as Al-Zn have unequal volume ratios as it has been explained.

### 1.7 Ternary alloys

Ternary alloys have been studied for directional solidification since the mid-1960's. <sup>(8)</sup> Kerr et al., <sup>(9)</sup> found that the morphology of their Pb-Cd-Sn eutectic specimens was completely lamellar with an ABCBA type of structure. (A, B, C, refer to Sn-rich, Pb-rich, Cd-rich phases respectively). Cooksey and Hellawell <sup>(10)</sup> met three different three-phase arrangements during their investigations: Three lamellar

phases of the type ABCBA as previously mentioned--two phases lamellar with the third phase occurring as more or less regular fibres--three phases completely irregular. Ho-Quac-Bao<sup>(11)</sup> with Cd-Pb-Sn and Garmong with Al-Cu-Mg<sup>(12)</sup> observed the breakdown of planar interfaces into cells and dendrites when composition moves away from the ternary eutectic Cd-Sn and Al-Al<sub>2</sub>Cu. A considerable amount of work has been devoted to "pseudobinary" eutectics which are systems with a composition lying on the saddle point of a eutectic line of two-fold saturation, especially when a carbide is the fibrous phase:--Co-Cr and Ni-Cr solid solutions reinforced by monocrystalline fibres of TaC,<sup>(13)</sup> --composites in the ternary system Cr-Co-C consisting of a cobalt matrix containing some dissolved chromium and an aligned fibrous dispersion of (Cr,Co)<sub>7</sub>C<sub>3</sub>.<sup>(14)</sup> Other pseudobinary systems such as NiAl-Cr,<sup>(15)</sup> Ni<sub>3</sub>Al-Ni<sub>3</sub>Cb,<sup>(15)</sup> and Cd<sub>3</sub>As<sub>2</sub>-NiAs<sup>(17)</sup> have been studied in detail.

## 2. Control of Eutectic Microstructures

### 2.1 Nucleation and growth

A wide range of binary metallic or ionic salts, eutectic mixtures assume lamellar structures when they are frozen unidirectionally. Cooksey, et al.<sup>(18)</sup> consider how the solid liquid growth profile determines the distribution of phase in the solid and hence how microstructures may be controlled by the freezing variables rate and temperature gradient. Binary systems present cases (I) where phases nucleate heterogeneously to give duplex nuclei and cases (II) in which phases nucleate independently from the liquid. Preferred epitaxial orientations between constituents would occur during nucleation of type (I). Two types of growth are distinguished. Either the phases grow at a given rate with similar

undercoolings (Case A) or with dissimilar undercooling (Case B). Therefore, there are four ways for a binary eutectic reaction to proceed, involving mechanisms I-A or B, or II-A or B. Figure 2 shows a diagrammatic representation of eutectic growth. Actual growth profiles exhibit a variety of complex curvatures. Distinction between A and B has some flexibility. It is expressed in terms of the lead distance,  $d$ , or its ratio to the interphase opening  $\lambda$ .

## 2.2 Short-range cooperative growth

For a short-range cooperative growth, the ratio  $d/\lambda$  would not exceed much unity. Also  $\lambda$  must be uniform. This is achieved only if the phase distribution is one of parallel lamellae or close packed fibres.

The difference  $\delta\Delta T$  between the total undercoolings for each phase,  $\Delta T_\alpha$  and  $\Delta T_\beta$  determines the magnitude of  $d$ , such that

$$d = \delta\Delta T/G, \quad (\text{Eq. 1})$$

where  $G$  is the temperature gradient. A spatial arrangement or growth profile which decreases the total undercooling below the mean value corresponding to independent growth of each phase is termed "cooperative".

Then  $\Delta T$  is very much smaller than either  $\Delta T_\alpha$  or  $\Delta T_\beta$ . Kinetically similar materials rejecting solute at similar rates are likely to present a freezing profile similar to type A. Then the solid interfacial energy is the most important factor controlling the phase distribution. It is only when  $\lambda$  is very large that magnitude of the solid liquid surface energies may override that of the solid boundaries. The microstructure produced by a growth profile of type B is determined primarily by the growth habit of the leading phase. The second phase simply fills intermediate space. The importance of the solid surface energy is

less than for a profile of type A. When  $d/\lambda$  is not very large the leading phase may not project sufficiently far into the liquid either to preclude cooperative growth or permit the development of a well defined crystallographic habit. Then it is likely that this situation favors a fibrous structure. Anyway, the leading phase is the more anisotropic since it does not tend to grow laterally. Formal treatment of solute distribution and interfacial energy will be found in references (19) and (20).

### 2.3 Discussion of the Freezing Variables

2.3.1 These variables are essentially the rate, the gradient and the impurity content.

2.3.2 Rate. Binary (10), (21) and ternary (22) eutectic materials have their interphase spacing  $\lambda$ , related to the freezing rate R by a relation:

$\lambda = A.R^{-n}$ , where A is a constant and n an exponent about 0.5 (Eq. 2).

However values of n as low as 0.35 have been reported.<sup>(7)</sup> Maximum values of  $\lambda$  would approach 10 $\mu$  in metallic systems, 20 $\mu$  in ionic salts and still larger values in organic materials. As it will be explained later, sometimes it is difficult to produce two lamellar materials from the same eutectic with their interlamellae spacings in a given ratio, because the theoretical rates as found from the previous equation would correspond to different structural stability domains in the plane (R,G), if G is kept constant. Section 2.4 presents a program of experiments for investigating the types of microstructures obtained with various rates and gradients. At very slow rates, the eutectic structure degenerates.

### 2.3.3 Thermal gradient in liquid

Recalling the relation (Eq. 1),  $d = \delta(\Delta T)/G$ , of section 2.2, where  $d$  is the lead distance and  $\delta(\Delta T)$  the difference between the total undercoolings of each phase, an inverse linear dependence is expected between  $d$  and  $G$  for a given freezing rate and phase distribution. Nucleation problems make it desirable to take  $G$  as high as possible, as explained in section 6-1. On the other hand, the  $G/R$  ratio is an important factor. Its influence on the microstructures is emphasized in the next section. Depending on the type of structure wanted and the impurity content  $G$  will be adjusted to some convenient value as found from the program of experiments.

### 2.3.4 Impurity content

2.3.4.1 Two degenerate forms of the lamellar structure are now known to be caused by impurities; these are the colony structure and the rod structure.<sup>(23)</sup> In fact, parallel growth of lamellae (or rods) occurs in a pure eutectic during unidirectional solidification when the growth front is planar. Effects of impurities on the relative values of solid-solid, and solid-liquid interfacial energies are difficult to forecast. Solute effects such as described by the relevant phase diagrams when they exist are more tangible. Two possible effects are to be considered depending on the scale. On a fine scale, different rates of solute rejection from each eutectic phase might cause different degrees of solute undercooling. However, selective doping impurities did not produce such a discernible effect. Such insensitivity to impurity content can be explained by pointing out that the rates of rejection of a third component from each eutectic phase are some order of magnitude lower than for the two binary components.

2.3.4.2 Colony structure. On a larger scale, the combined solute rejection of the impurities from all solid phases can produce colonies, which grow with a cellular interface. Bending of the lamellae results. Therefore, the production of aligned lamellae requires a sufficient purity. Yue<sup>(24)</sup> derived an equation describing the constitutional supercooling under the combined effect of concentration and temperature gradient

$$G(0)/R \leq m(C_0/D)[(1/k_0 - 1) + (1/k_0)(T_1 - T_0)(D'/K)] \quad (\text{Eq. 3})$$

where  $G(0)$  is the temperature gradient in the liquid at the solid-liquid interface,  $R$  is the solidification rate,  $m$  is the slope of the liquidus, (see Fig. 3),  $C_0$  is the initial impurity content,  $D$  is the diffusion coefficient,  $k_0$  is the equilibrium distribution coefficient,  $T_1$  is the temperature of the heat source,  $T_0$  is the temperature of the interface,  $D'$  is the thermal diffusion coefficient, and  $k$  is the thermal diffusivity. If, furthermore, assumption is made that  $T_1 = T_0$ , the criterion reduces to

$$G/R < m(1 - k_0)C_0/Dk_0 \quad (\text{Eq. 4})$$

which is the criterion for the onset of constitutional supercooling proposed by Tiller, Jackson, Rutter and Chalmers.<sup>(25)</sup> Weart and Mack<sup>(26)</sup> attribute the formation of cellular structure in eutectic mixtures to a layer of constitutionally supercooled liquid generated at the advancing interface by the simultaneous rejection of an impurity by the two phases of the eutectic mixture. The constitutional supercooling is relieved by cell formation and the resulting transverse diffusion of the impurity.<sup>(19)</sup> Another expression derived by Cline<sup>(27)</sup> may predict a range of stability wider than predicted by Eq. 4:



$$G/R = \frac{1}{2} (K_s/K_l + 1) [(C_o - C_1)m^x/D + B \bar{C}_o] \quad (\text{Eq. 5})$$

where  $K_s$  is solid thermal conductivity,  $K_l$  is liquid thermal conductivity,  $m^x$  is the effective binary liquidus slope,  $C_o - C_1$  is the difference in binary initial and interface composition,  $B$  is a positive constant, and  $\bar{C}_o$  is the ternary impurity content.

Plots of  $G/R$  versus antimony content or zinc content have been made by G. Garmon<sup>(28)</sup> for Pb-Sn eutectics. The structures obtained show that there is a critical  $G/R$  ratio which is a linear function of  $C_o$ . Similar experiments had been conducted by Yue, et al.,<sup>(24)</sup> with the Al-Al<sub>2</sub>Cu eutectic composite. Their results showed that the  $(G/R)$  ratio above which cellular structure is eliminated is proportional to the impurity content. As a conclusion, when cellular structure is present, the operator either will decrease  $R$  or increase  $G$ , if the impurity content is kept the same. The other alternative is to proceed to sufficient purification.<sup>(29)(30)</sup>

2.3.4.3 Rod structure. According to Chadwick,<sup>(30)</sup> the rod structure replaces the lamellar structure when an impurity has sufficiently different distribution coefficients for the two solid phases. Then the lamellae of one phase should grow into the liquid ahead of the other while the lamellae of the lagging phase would break up into small cells surrounded by the other phase.

2.3.4.4 Intermediate structures of colonies. They are lamellar in the middle and rod-type on the edges. The distribution coefficients for the two solid phases are nearby equivalent at low concentrations of an impurity. However, when concentration increases there is an increasing

difference between them. As a result, the structure is lamellar in the middle part of the cells where the concentration is low. The rod type structure appears when the difference between the distribution coefficients has reached a sufficient value. The adding of 0.1% tin to the lead-cadmium eutectic gives the intermediate structure.

## 2.4 Program of experiments

2.4.1 Experimental programs in view of recognizing the influence of different variables are described in Refs. (7) and (18). In one program<sup>(7)</sup> eutectics were prepared from metals having impurity contents ranging from 1 to 100 ppm (see section 3). The materials were re-melted in horizontal graphite boats of 8 mm bore and 25 mm length in evacuated silica or glass tubes or under an argon atmosphere. The rates of withdrawal and the true freezing rates were supposed to be equal along the central portions of the specimens. Rates from 0.05 to 20 cm/h were used and imposed temperature gradients were from 30 to 40°C/cm. A similar campaign was conducted at Berkeley, Department of Materials Science and Engineering for the Al-Al<sub>2</sub>Cu eutectic. The thermal gradients were from 20 to 55°C/cm and the rates from 0.15 to 22.5 cm/h. The impurity content was not estimated but supposed to be the same in identical conditions. In another program,<sup>(18)</sup> alloys did not contain more than 5 ppm of impurities. Specimens 12-15 cm long and 1 cm in diameter were frozen in recrystallized alumina tubes by withdrawal vertically downwards from furnaces at controlled temperatures. High temperature gradients up to 120°C/cm were achieved by adjusting the position of a water cooled copper cylinder surrounding the refractory tube. Low temperature gradients down to 1°C/cm were obtained by setting furnace

temperatures only a few degrees above  $T_E$ . Macroscopic growth fronts were found planar except in the immediate vicinity of the refractory container.

2.4.2 Types of microstructures met. The types of structures which may be observed in any given eutectic may be divided in three classes<sup>(7)</sup>: (1) unmodified or typical, (2) modified with impurity cell formation, and (3) modified without cell formation. The unmodified structures are defined as those found in perfectly pure eutectics frozen under steady state conditions. These structures are also observed in impure materials below certain freezing rates and/or above limiting temperature gradients (see sections 2.3 and 4.2). Of the modified structures, those due to impurity cell formation are easy to recognize. Modification without cell formation is not an impurity effect since it occurs in alloys prepared from materials having less than 5 ppm of impurity.<sup>(7)</sup> Degenerate structures caused by the breakdown of the lamellar arrangement would occur at freezing rates less than 5 mm/h. Examples of these degenerate structures have been observed in Al-Al<sub>2</sub>Cu and Al-Zn eutectics where the lamellar arrangement becomes wavy and is less obviously related to the freezing direction. The Al-Ag<sub>2</sub>Al eutectic shows a degeneration which begins by step formation which causes lamellae to become serrated. In LiF-NaF and Al-Ag<sub>2</sub>Al systems the distribution becomes fibrous whereas the high volume fractions would have been expected to forbid this type of structure. These phenomena would be connected with a change in diffusion conditions.

2.4.3 Range of stability of the different microstructures. Schematic representations such as that of Fig. 4 are used. A transition between lamellar and degenerate structures is expected to be found at some low freezing rate. It would depend only on the freezing rate. Generally, one program will not illustrate more than one transition in growth mechanisms for any one alloy. In a system Al-CuAl<sub>2</sub> constituted from very pure materials, the transition from lamellar to degenerate is easily observed. If some impurity content exists, the transition from lamellar to cellular structure will be observed instead. (31)

The Al-Al<sub>3</sub>Ni eutectic has a lamellar to fibre transition easy to produce. It requires a high freezing rate and a low temperature gradient. The partitioning of individual coolings and hence the total undercooling is sensitive to both of these variables. Breakdown to noncooperative or independent growth will occur for such systems as Al-Li, Fe-C which involve metallic with covalent solids. At some upper limit of rate or lower limit of gradient, one phase is obliged to renucleate repeatedly owing to termination of growth of this phase.

2.4.4 Defects such as bands with an indication of the degree of banding may be represented also on the schematic diagram.

### 3. Purity Requirements for the Materials

#### 3.1 Commercial materials

In order to avoid cellular breakdown of the interface it is recommended to use the purest materials available rather than to adjust only the (G/R) ratio. However, materials obtained commercially in a very pure form do not guarantee that an eutectic colony microstructure will not form. For instance, Kraft and Albright used high purity

copper, estimated 99.999 % Cu and spectrographic aluminum rods, having impurities other than copper estimated to be Zn-15 ppm, Mg-10 ppm, Fe-3 ppm, Na-2 ppm, Cd-1 ppm, and Mn less than 1 ppm. These materials were melted in a stabilized zirconia crucible in a vacuum induction furnace under a pressure about  $10\mu$  of Mg. The melt was superheated to assure mixing, cooled to  $780^{\circ}\text{C}$  and cast. The casting was allowed to solidify under vacuum. The specimens were remelted in graphite crucibles lowered through a stationary coil and water quenching system. Oxidation of melt and graphite crucibles were minimized under an atmosphere. In all specimens they noted either a tendency toward colony structure or a very pronounced colony structure in the last one or two solidified centimeters. Indeed, impurities with a distribution coefficient less than one were rejected toward the end, thereby inducing colonies.

A better material can be obtained by dropping the last portion and repeating the operation. However, some possibilities of contamination still exist. Pronounced colony structures were found in the specimens otherwise free of them in the vicinity of a thermocouple head. The melt had been contaminated in this area by limited solution of one or more of the elements. The materials can be zone refined. Another process uses zone leveling. It is the name given by Pfann<sup>(32)</sup> to a group of processes in which the motion of a molten zone along the sample produces a large region of uniform composition, as distinct from zone refining in which the composition varies from one end to the other. The zone leveled end can be removed and grown unidirectionally. In practice, preliminary tests with a given material and a given equipment will allow determination of the degree of purity necessary for growing large single grains of eutectic.

### 3.2 Contamination

Two kinds of contamination must be distinguished<sup>(33)</sup>: that caused by a solid, such as the crucible or the boat, and that caused by the atmosphere. Contamination from the crucible will depend on the chemical characteristics of the substance under consideration, and on the temperature that is required. As the temperature is raised, the problem becomes increasingly severe and that is the reason why the floating zone has been developed in the case of the single crystals with high melting points. Contamination by the atmosphere is more easily controlled by using a vacuum or an inert gas such as argon.

## 4. Temperature Requirements

### 4.1 Temperature setting of the furnace

When a high gradient is wanted, the temperature setting will be somehow higher than the melting point. For instance, it will be 900°C instead of  $T_E = 548^\circ\text{C}$  (Al-Al<sub>2</sub>Cu) for a given horizontal furnace without a special cooling device or thermo-reservoir for adjusting the gradient. When extremely low gradients are wanted for a research the furnace settings will be only a few degrees above  $T_E$ .

### 4.2 Temperature stability

From the relation

$$dT/dt = G \times R, \quad (\text{Eq. 6})$$

the rate of temperature change in the melt at the interface is the product of the growth rate and the temperature gradient. A temperature stability of 1°/mm with  $G = 20^\circ\text{C}/\text{cm}$  can create growth rate fluctuations of 3 cm/h while the preselected rate is only 0.6 cm/h.

#### 4.3 Temperature controller

4.3.1 Modern electrical controller-recorders provide modulated control on a closed feedback circuit.

4.3.2 The following types of control action are commonly encountered:

- (1) The simple on-off action which demands power for an error signal below the set point,
- (2) The proportional action which produces an output signal proportional to both the magnitude and the time duration of the deviation from the set point,
- (3) Reset or integral action which produces an output signal proportional to both the magnitude and the time duration of the deviation from the set point, and
- (4) Rate or derivative action which produces an output signal proportional to the rate of temperature change and is in a direction that will oppose the change.

4.3.3 Packaged control units use these actions to provide three different kinds of output signals for controllers:

- (1) Modulation of output current (CAT)
- (2) Modulation of duration of contact closure (DAT)
- (3) Modulation of electric drive unit position (PAT)

The CAT units use a magnetic amplifier or a silicon controlled rectifier which supplies the control signal depending on the output current intensity. They are a rapid and sensitive means for adjusting large or small power inputs to the electrical furnace. Description of DAT and PAT units will be found in Ref. (34). One problem to be solved is the mating of any of these control units with a given furnace system in view of obtaining the optimum setting for each of the control functions.

4.3.4 As an example, a CAT system controls the temperature of an horizontal furnace operated in the Department of Materials Science at Berkeley. Two thermocouples (Chromel-Alumel) in parallel measure the temperature of the same point near the center of the furnace. One duplicates the electromotive force collected by the second. If one thermocouple fails, the power is shut off. If temperature rises above some predetermined limit between zero and 2000°F, the power is also turned off.

The electrical power is progressively raised by adjusting manually the current to keep it constant, while voltage is automatically increased at each adjustment. When the steady state is reached, control is switched from "MANUAL" to "AUTO". Automatic control depends on a preselected combination of proportional control, reset and rate time action. For adjusting the controller to a typical operation, generally the proportional band is adjusted first by decreasing it from a starting value of say 50%, until a cyclic record happens and then increasing it until the cycle disappears. Rate action is then introduced and the proportional band adjusted again. At last, a not too large reset rate will be selected, because it would decrease the basic stability of the control action.

The following settings revealed to keep steady the temperature while the furnace was moving:

- proportional band: 10% of recorder scale
- rate time: 0.05 mm
- reset: 0.1 repeats/mm

(on a series 60 control unit built by Leeds & Northrup).



The spans of the Speedomax recorder are the following: 2-5-10-25-50 or 100 mV for 100 graduations. The 50 mV span is chosen if the temperature to be obtained corresponds to an emf: 29.14 mV or 37.16 mV.

When the record shows an emf at some mV below the setting, a lower span is selected while the complement of emf is taken on a potentiometer "ADD to ZERO". It is possible to add to zero 0-10-20-30-40-mV plus a voltage between 0 and 10 mV taken on a "vernier" which can be appreciated to 0.01 mV. Records showed that the setting point was kept constant during one day with fluctuations less than 0.02 mV.

#### 4.4 Choice of thermocouples

4.4.1 A number of selection factors must be considered. The following criteria will help for selecting a convenient solution. (35)

- The thermocouple can only indicate the temperature at the measuring junction.
- The insertion at a given point may change the temperature distribution.
- The type of thermocouple is largely determined by the temperature range of interest.
- Compatibility with the system environment varies depending on the atmosphere whether it is oxidizing, reducing, inert or vacuum.
- An appropriate protection tube may be used but it imposes a slower response rate.
- The depth of immersion must be sufficient to bring the thermocouple in good thermal contact with the system.
- Thermocouple size selection must be influenced by whether a steady state or a transient has to be measured. For this latter case, a smaller size may be required to achieve a rapid thermal response.

- A redundancy of thermocouples will be useful when early failure of a component requires a replacement. The replacement can be temporarily avoided.
- Mechanical stresses which might lead to early failure must be avoided.
- Magnetic fields or high pressures can change the emf.

#### 4.4.2 Most commonly used thermocouples

##### Type J - Trade name: Iron/Constantan

- elements: SAE 1010 steel is the positive element  
Cu 60 Ni 40 (constantan) is the negative leg.
- use : in oxidizing (400°C) or reducing environment (800°C)
  - not recommended above 800°C
- sensitivity: 50 $\mu$  V/°C at 0°C, 64 $\mu$  V/°C at 760°C.
- main advantage: low price

##### Type K - Trade name: Chromel P/Alumel

- elements: Ni90Cr10 (= 9 minor constituents) is positive; the negative element is 95% Ni, plus controlled additions of Al, Si, Mn, Fe and Co. Negative leg is magnetic at room temperature.
- use : The negative leg is susceptible to oxidation. Some alloys which are better oxidation-resistant have been developed.
- sensitivity: 40 $\mu$  V/°C

##### Type S - Platinum/Rhodium

- elements: platinum and platinum 90, rhodium 10
- use : limited by the strength of platinum at high temperatures

- up to about 1500°C in proper conditions

- type 20/5: Pt 80 Rh 20/Pt 95 Rh 5

type 30/6: Pt 70 Rh 30/Pt 94 Rh 6

type 40/20: Pt 60 Rh 40/Pt 80 Rh 20

can be used up to 1850°C

sensitivity: 5.5µV 1°C at 0°C and 11.5 µV/°C at 1000°C

advantage: for use in oxidizing atmospheres as well as in vacuum or inert gases

4.4.3 Thermocouple wires. Single wires are delivered either bare or insulated. Duplex wires are delivered with different types of insulation on each wire and overall. Upper temperature limits and other insulation characteristics must be consulted for the parts which will not be stripped. Standard sizes generally refer to the AWG gauge. Table II gives examples of temperature limits.

Table II. Examples of temperature limits in (°F)\*

Material	Couple condition	AWG					
		8	14	16	20	24	30
Iron/Constantan	bare		900	900	800	650	600
	protected		1100	1100	900	700	700
Chromel/Alumel	bare	2000	1700	1700	1600	1400	1300
	protected	2300	2000	2000	1800	1600	1500
Pt/Pt-Rh	protected				2800	2700	2400

\* (from catalog of Leeds & Northrup)

4.4.4 Thermocouple insulators. Catalogs specify the maximum wire size (AWG), the length (for instance, 18 or 24 inches), the outside diameter and the diameter of the hole. Single hole and double hole construction exist.

4.4.5 Protecting tubes and ceramics. In some cases, protecting tubes with one closed end, spun and welded on a disc may be used to provide protection against mechanical injury or against the corrosive action of some atmosphere. An alloy of iron with 28% chromium will undergo a maximum temperature of 2000°F. For higher temperatures, the envelope could be a ceramic.

4.4.6 Preparation of thermocouple. The convenient length of wire is taken from the coil and stripped if necessary. Next, it is carefully aligned. Then, the wire can be progressively and regularly advanced through the hole of the insulator until about one inch and 1/2 have gone through the other end. In the case of a round double hole insulator, the operation will be repeated for the second hole with the other thermo-material. Next, the two wires are twisted together on three turns and welded under proper flux on a special machine which provides a short pulse of electrical current. The outer part of the weld is dropped with a cutter. A similar operation is realized for the cold junction. Automatic compensation of room temperature or an ice bath (mixture of ice and water in a Dewar vessel) are generally used. When extension wires connect the thermocouples to the instrument, they must be of the same material as the couples. The circuit has to be broken at one point to allow a recorder of the emf to be inserted.

4.4.7 Selection of a recorder. The temperature range of interest is translated into a range in mV for the recorder, and the convenient scale is chosen. The zero and the damping are adjusted and the scale is calibrated with respect to a reference source. Speed of the chart depends on the rate of change; if one inch/hour is sufficient for a

steady state, the analysis of a transient thermal gradient moving at a speed of 4 cm/h may require a chart velocity of 4 in./h which allows one inch to represent a relative displacement furnace-crucible of 1 cm. For long duration operations, a record is the proof that temperature evolution corresponded to what was expected, and that appreciable fluctuations did not occur.

4.4.8 Calibration of thermocouples. The drift of the emf limits the life of the thermocouple. When calibration is needed, it is done by comparison with a thermocouple previously calibrated by a manufacturer at some fixed points (freezing points of Gold = 1063.0°C-silver = 960.8°C-zinc = 419.5°C). Only high accuracy measurements refer to primary standards (Pt-Pt90 Rh10) supplied with an NBS report of calibration.

## 5. Furnaces

### 5.1 Similarity with case of single phase materials

The problems encountered are similar to those for crystal growth of single phase materials.

5.2 Eutectics with melting points less than 1100°C. This section concerns only eutectics with melting points less than 1100°C. Schematically, the growth of homogeneous crystals is controlled by the movement of the melting point isotherm through the specimen.<sup>(36)</sup> There are three basic methods: (1) movement of the furnace, (2) movement of the sample, and (3) movement of the isotherm by temperature control (see Fig. 5). The first method is often the simplest to carry out. It does not create any vibration in the melt but Gilman points out that small vibrations would not have any significance when the movement is smooth.

The second method is conveniently used with large furnaces or high frequency heating systems. The third method offers some advantages when very slow growth rates are required.

A temperature programmer replaces the furnace moving equipment.

### 5.3 Simple physical arrangements

The designer of a project has to choose between two simple physical arrangements. If he decides for an horizontal method, boat-shaped molds will be used. Seeding is relatively easy, but transverse cross sections of the materials are asymmetric. Differences in thermal conditions above and below the melt are difficult to avoid (see Fig. 9). Vertical methods are expected to produce more symmetrical materials in more uniform conditions, but seeding is more difficult and expansion on solidifying may create strain. A soft mold method has been proposed to prevent this effect. The term "Bridgman method" is used when the melt is lowered through the furnace. Stockbarger exploited the method from 1936 to 1949 after Bridgman (1925) and its name is associated (see Fig. 6).

### 5.4 High melting points eutectics

5.4.1 It is admitted that the Bridgman technique has been most useful for growing crystals of metals below 1500°C. The floating zone melting technique is recognized as better between 1500°C and 3400°C.<sup>(37)</sup> See Fig. 7. It has been used for such eutectics as Fe-C system ( $T_E = 1155^\circ\text{C}$ ), Ni-C and Fe-C-Si.<sup>(38)</sup> The need for a container is eliminated by use of a molten zone established between two vertical cylindrical rods. Electron beam melting would afford better control over zone length than either induction or radiation heating.<sup>(38)</sup> The

energy density input is higher. Scattering of electrons is avoided by generating the beam and melting in vacuo.<sup>(39)</sup> The initial vacuum in the working chamber must be as low as about  $10^{-6}$  Torr for successful melting. It is the principal disadvantage. The electron emitter is commonly a simple ring filament in tungsten surrounding the specimen. Reflection plates in tantalum grounded or biased help in focusing the beam. The sample is under a bias voltage. Control of temperature is realized by controlling the bombardment current. Either the filament temperature or the potential difference between anode sample and cathode filament are adjusted. The equipment is described by Bakish.<sup>(40)</sup>

#### 5.4.2 Another method is the hollow cathode or cold-cathode technique.

This has been discussed by Class, et al.<sup>(41)</sup> Its advantage when compared with the electron bombardment technique is that it can be operated at pressures of approximately 1 mm while the latter requires at least  $10^{-4}$  mm Hg, thereby creating frequent problems of compound decomposition.

### 6. Thermal Gradient Requirement

#### 6.1 Cases of small and large gradients

Too small a thermal gradient along the crucible is a difficulty commonly met in the Bridgman-Stockbarger method. Then, an appreciable supercooling exists in the melt. Even, it might happen that the whole sample could be below the melting point before nucleation of the solid phases. Large thermal gradients cause nucleation to occur before the entire sample is below the melting points, thereby creating conditions of controlled growth as the  $T_E$  isotherm moves through the sample.

#### 6.2 Temperature profile of the furnace

It is wise to record the temperature profile at some point near

the crucible for a constant rate and a constant temperature setting at the control of the furnace. The displacement of the furnace is noted at regular intervals of time directly on the emf record. These informations are sufficient for drawing the temperature profile of the furnace, giving  $T$  as a function of displacement,  $x$ . Reproducibility of these profiles will be checked in the presence and the absence of charge. Radiation shields and chillers near the charge affect the profile to some extent. The thermal gradient in liquid is estimated from  $dT/dx$ .

### 6.3 Thermal gradients used in Bridgman-Stockbarger growth

Either the gradient is forced to move through the melt by cooling the whole furnace (it is the third method of section 5.2) or a resistance wire wound furnace has a relative motion with respect to the crucible. This method provides a different gradient. However, it is advantageous to increase the gradient by suspending the crucible between two temperature reservoirs. The upper reservoir is maintained at a given temperature above  $T_E$ , while the lower reservoir is maintained at a rather uniform temperature well below  $T_E$ . The two reservoirs should have a minimum of thermal coupling between them. Isothermal conditions in the two regions are better obtained if the inner furnace walls have a high thermal conductivity. A reflecting baffle (a Pt sheet) with a passage just sufficient for the crucible separates the two zones in some equipments.

### 6.4 Horizontal method

The same considerations of sections 6.3 apply. (See Fig. 8).



## 6.5 High temperature growth

Lemkey and Salkind report<sup>(42)</sup> that they prepared whisker-reinforced refractory metals by unidirectional solidification of Nb-Nb<sub>2</sub>C and Ta-Ta<sub>2</sub>C eutectics using electron beam zone melting. The temperature gradient was estimated to be in the order of 900-1000°C/cm.

## 7. Molds

### 7.1 Mold materials

7.1.1 What is wanted is a mold that does not react in order to avoid spurious nucleation. The fact that an eutectic might have different wetting characteristics when clean than with a thin oxide coating must be considered. A listing of the most commonly used materials follows.

7.1.2 Pyrex has its softening point about 600°C. In some cases, a coating of Aquadag (colloidal graphite) alloy is applied to avoid sticking. Its prime advantages are that it is easy to fabricate and it is inexpensive. For cleaning, a solution of 5% HF, 33% HNO<sub>3</sub>, 2% Teepol and 60% water may be used.

7.1.3 Vycor which has a softening point of about 1000°C is much more expensive and not so easy to fabricate.

7.1.4 Silica softens at about 1200°C and is chemically inert (of the common acids, only HF attacks it). It is available in very high purity forms such as Spectrosil or synthetic silica. Typical analyses give ppm of Al, Sb, As, B, Ca, Cu, Ga, Fe, Mn, P, K, and Na. For cleaning, a solution 1 HF with 10 HNO<sub>3</sub> may be used with soaking for 1 hour and rinsing in de-ionized water for the same period. It can receive a carbon coating.

7.1.5 Pyrex, Vycor and vitreous silica are limited to low melters.

Their advantage is that they permit visual observation of the growth process in a suitably designed furnace.

7.1.6 Alumina is stable to very high temperatures. Prefabricated forms can be obtained after firing with convenient binders. It is available in high purity.

7.1.7 Graphite may be used to at least 2500°C in non-oxidizing atmospheres and for materials which do not form easily carbides. It is obtainable in very high purity. Usually, it is considered necessary to sweep an inert gas through the furnace when graphite crucibles are used. Graphite is easily machined and a hard surface can be obtained when the grain size is convenient. Cleaning is provided by a final high temperature firing. Compared with the thermal conductivity of Pyrex (0.002 CGS) - of Vycor (0.003), - of Silica (0.003), Graphite has a high thermal conductivity of 0.4 (at 0°C) to 0.2 (at 800°C). Its use is not restricted to charges with a melting point above 1000°C and it is sometimes preferred for relatively low melting point eutectics. Some grades have a maximum ash content of 10 ppm with B, Mo, Ca, Na each less than one and traces of Mg and Si.

7.1.8 Other mold materials such as pyrophyllite (an aluminum silicate, machined and then fired at 1050°C), stainless steel, silicon carbide, aluminum nitride and boron nitride might be considered for some applications.

7.1.9 Soft molds are used to prevent strains in materials that wet the crucible. (43)(44) For instance, a very thin easily deformable platinum container, supported or not by a stronger external crucible

deforms as the material contracts. Therefore, no strain is introduced in the grown material.

## 7.2 Shape of the crucible

It depends on the type of technique, whether the furnace axis is horizontal or vertical. Open boats (Chalmer's method) are used generally with the horizontal furnace. It is possible to place a seed in the crucible tip. The temperature profile must be arranged so that it does not melt it. Visual observation is not possible for most of the systems. Using a seed suppresses the need for complex crucible shapes.

Vertical furnaces require cylindrical crucibles.<sup>(45)</sup> Seeding is relatively more difficult because of difficulties of orientation. Expedients used for causing one of the crystallites to dominate the solid liquid interface—in the case of single crystals growth might be tried for eutectics—crucibles with a conical tip, with a capillary tip, with a conical tip connected to the main volume by a capillary, with many bulb capillary pairs. The crucibles can be closed when moderately volatile compounds have to be grown.

## 7.3 Size of the crucible

- Vitreosil, vitreous silica - horizontal boats, from  $L = 3$ ,  
 $W = 5/8$ ,  $h = 3/8$  to  $L = 6-3/10$ ,  $W = 3/4$ ,  $h = 5/8$  (inches) - vertical  
crucibles from  $D = 1-5/32$ ,  $H = 3-1/2$ , to  $D = 5-13/16$ ,  $H = 10-5/8$   
Supplier: Thermal American Fused Quartz Co., Montville, N. J. 07045.

- Alumina, AD-999, horizontal boats, up to  $L = 100$ ,  $W = 20$ ,  
 $h = 13$  (mm) - AD-998 up to  $L = 137$ ,  $W = 27$ ,  $h = 21$  (mm)

- cylindrical vertical crucibles  
from  $D = 12$ ,  $h = 25$  to  $D = 178$ ,  $h = 11$  (mm)

Supplier: Coors Porcelain Company, Golden, Colorado.

- Alundum - horizontal boat, up to  $L = 10$ ,  $W = 1$ ,  $h = 9/16$  (inches)

Supplier: Norton-Worcester

- cylindrical crucible

from  $D = 1-1/8$  -  $H = 15-1/2$  to  $D = 3-1/2$  -  $H = 19-1/2$

The same sizes are supplied by Norton in Thoria, fused stabilized zirconia and silicon carbide.

- Graphite,  $L = 11\ 3/4$ ,  $W = 1\ 1-15/16$ ,  $h = 1-1\ 31/32$  (inches)

Supplier: Ultra Carbon Corporation

#### 7.4 Preparation of charge

It seems appropriate to recall that the initial charge has to be clean in order not to introduce contamination which would be difficult to remove later. It may happen that the as cast vacuum melt - rods do not fit to the crucible size. Then convenient pieces of material have to be machined in a good surface state which facilitates further cleaning with an alcohol solution. Differential mechanical stresses will be avoided if the charge is uniformly spread. Liquid metal viscosity and surface tension could delay equal distribution of the material. A seed is sometimes introduced at one end of the charge.

#### 7.5 Lifetimes of crucibles

They are statistically variable. Fabrication defects or random events may shorten their lives. Each accident will be noted and analyzed. Operators have an interest to avoid shortage of crucibles. High temperature gradients are expected to generate thermal stresses. This fact should influence the selection.

## 7.6 Thermal convection in horizontal boats

Utech et al., have studied the thermal convection in open horizontal boats containing molten metals subject to an axial temperature gradient.<sup>(46)</sup> The Prandtl number ( $Pr = \nu/\alpha$ , where  $\nu$  is kinematic viscosity and  $\alpha$  the thermal diffusivity) is a dimensionless parameter which would classify the convective behavior of the melt. The authors gave an approximate representation of the flow pattern. Carruthers and Winegard show that the degree of thermal convection is not only dependent upon the horizontal temperature gradient but also upon differences in the rate of heat transfer across the liquid in the lateral or vertical direction.<sup>(47)</sup> Utech and Flemings report the effect of a magnetic field. Temperature fluctuations as a result of turbulent thermal convection are suppressed by magnetic flux densities as low as 500 gauss.<sup>(48)</sup>

## 7.7 Seeding

A little piece of eutectic material coming from a single grain zone can be used as a seed. Knowledge of the orientation of plates and crystallographic planes is supposed to be helpful.

## 8. Atmosphere Requirement

### 8.1 Possibilities

Most of the equipment foresees two possibilities: a vacuum system and inert gas atmosphere. Generally it is possible to switch from one to the other.

### 8.2 Vacuum system

A mechanical pump will "rough" the vacuum to about  $10\mu$  (10 millitorr). The diffusion pump must be cooled by putting the water and liquid nitrogen on. An automatic level controller of liquid nitrogen will function

periodically. When  $10\mu$  are obtained, the heater is started. It takes about thirty minutes. The two pumps must be put actually in series and never in parallel. When stopping the vacuum system, the heater will be turned off first. One waits until it is cold before shutting off the water, liquid nitrogen and the mechanical pump.

### 8.3 Neutral atmosphere

8.3.1 A few psi (3 to 5) above the atmosphere pressure are considered sufficient. First, the air contained in the tube is eliminated and progressively replaced by the gas, argon, for instance. For that, the valve of the argon tank is open. The manometer indicates a pressure between 800-1500 psi depending on the previous consumption. No gas is allowed to flow. The pressure through the regulator is progressively adjusted from 0 to 5 psi. Now, the operator opens the valves at both ends of the tube. He opens slightly the valve located just after the flowmeter and allows the flow between 5 and 10 CF/H. Then argon will replace air in the tube for some time calculated from the flow and the volume of the tube for a given number of renewals. When this number has been reached, the external valve is closed and pressure builds up in the tube (see Fig. 9).

8.3.2 Then, the system has to be checked against possible leakages of gas. For that, the internal valve of the tube is closed and the pressure indicated by a manometer connected to the tube will be noted after one day. If the tube does not keep constant pressure, the cause of the leakage has to be found. Pressure is reinstated in the incriminated volume. A special liquid, Leak-Check, will help for detecting the leak by exhibiting growing bubbles at some point. Such spots as the passage

of thermocouples need a special surveillance. It will be wise to wait again for 24 hours and to observe constance of pressure before starting a melting operation.

9. Rate Requirement

9.1 Range of growth rates

A range of growth rates must be available since acceptable microstructures exist only in some domains of the plane G, R.

9.2 Adjustment of the speed

Generally, it is possible to obtain continuous adjustment of the angular speed of a D.C. electrical motor, through excitation, for instance, within a very limited ratio. Since a drastic reduction is needed, in practice for attaining the low rates necessary to achieve the critical G/R ratio, a speed reductor will be inserted into the mechanical transmission.

9.3 Typical transmission for an horizontal furnace

A typical transmission used in conjunction with an horizontal furnace is now described. The D. C. electrical motor has the following characteristics: 115 D.C. volts, 0.28 Amp., RPM: between 0.20 and 0.49 depending on excitation,

Duty: continuous, Manufacturer: Bodine Electric Company, Chicago.

A power supply fed under A.C. voltage delivers the direct current to the motor which activates a speed reductor built by InSCO Corporation.

The following reductions (1/Red) are available: 1/1, 1/2, 1/5, 1/10, 1/20, 1/50, 1/100, 1/200, 1/500, and 1/1000. Mechanical power is

transmitted from the motor to the gear box and from the gear box to a large pulley  $P_1$  by means of rubber belts.

The pulley on the gear box primary shaft has a diameter 2.75 times larger than that of the electrical motor.  $P_1$  has a diameter four times larger than that of the pulley on the secondary shaft of the speed reductor. Then, RPM1 of  $P_1 = (1/(2.75 \times 4 \times R)) \times \text{RPM0}$  where RPM0 is the number of RPM of the electrical motor. Pulley  $P_2$  on the same shaft as  $P_1$  has a diameter of 2 inches. A stainless steel wire pulls on the horizontal furnace between  $P_2$  and a similar pulley (see Fig. 9).

The linear velocity of the furnace is calculated from

$$V_L = 1R \times 2 \times \text{RPM1}, \text{ inches/mm or}$$

$$V_L = 1R \times 2 \times \text{RPM1} \times 2.54/60, \text{ cm/sec or}$$

$$V_L = 1R \times 2 \times \text{RPM1} \times 2.54 \times 60, \text{ cm/hour.}$$

#### 9.4 Vertical design

Crucible is attached to a wire and chain transmission activated by a clock motor (supplied by Cramer Division of Giannini Control Corporation, Old Saybrook, Conn., and Automatic Timing and Controls, Inc., King of Prussia, Pa.). The accuracy depends on the average line frequency of the A.C. source, since the clockmotor is a synchronous motor and, if line frequency is maintained to much better than  $\pm 0.1\%$  over one day, however, short term variations are common. As a result, constancy of rate is no better than  $\pm 0.1\%$  over several hours. The motors have speeds from a fraction of revolution up to many revolutions per hour. Suitable size gears attached to sprocket of clock motor activate the chain. A counterweight reduced the torque and produces a condition of near mechanical equilibrium. Some transmissions are protected against vibrations, or accidental crucible displacement by



transmitting motion through a rigid support. (49) Instead of lowering the crucible, a worm drive can be used for raising the furnace. (50)

## II. EVALUATION OF EUTECTIC MICROSTRUCTURES

### 1. Preparation of Sample

After solidification, each ingot is extracted carefully from the mold. It seems necessary to create distinctive marks with an electric marker at the head and at the tail. Operation number also may be written. Generally, the microstructure is evaluated on at least two sections: a longitudinal section A parallel to the direction of growth (parallel to the bottom of crucible in case of a horizontal boat; a transverse cross section B, perpendicular to the direction of growth.

Sometimes, a third section C, longitudinal and perpendicular to the first may be useful when orientation is not clear (see Fig. 10). Current practice of metallography requires that size of samples does not exceed about 15 x 10 x 10 mm. However, valuable information could be obtained through examination of the entire ingot on section A. Thus, after convenient polishing and etching, it would be possible to appreciate with an optical controller whether extended regions of the material belong to single eutectic grains, or not. Then, conclusions for sampling from one of these grains could be drawn. At the limit the ingot would be one single eutectic grain, if the growth technique is successful, except at the end where impurities are supposed to concentrate, thereby creating colonies. Anyway, this part would be dropped. When sampling, one has to decide about optimum location of cuts. Generally, the sample has the shape of a parallelepiped. Different solutions exist for machining the material. Some possibilities are evocated below:

- "spark cutters," such as SERVOMET<sup>51</sup> do a fine work but the sample must be conductor of electricity. Duration of operation is rather long.

- milling machines with a convenient sprinkling or cooling device, at the proper speed.

- cut-off saw (supplied by Di-Met) with diamond cutting wheels under sprinkling. The method is tested in a shielded transparent enclosure before being repeatedly used for a series of specimens. A graphite block can be used as a support which undergoes slight cuts without harmful consequences. Epoweld 8173 (available from Hardman, Inc.<sup>52</sup>) or Duco Cement (from DuPont) hold some direction of reference on the specimen; for instance, the direction of growth, perpendicular to the wheel. Next, Epoweld or Duco are removed with an organic solvent boiling at moderate temperature for instance.

## 2. Characterization of the Material

### 2.1 Metallographic techniques for optical microscope.

2.1.1 Mounting the specimen in thermal plastic mounting materials such as Bakelite, Lucite, Plexiglas, will facilitate polishing since these materials are relatively hard after molding. They polish well with a minimum amount of clogging of the emery papers. They are not attacked by the usual etching reagent. They are electrically neutral. They should not be used in mounting soft materials, such as tin or lead because the pressure required during heating may deform the specimen. Bakelite is supplied in a variety of colors;<sup>53</sup> Lucite is transparent. Description of a bakelization operation which is commonly used follows now. The face to be polished is laid on the top of a vertical piston in a Presto-Press machine. Then the piston is lowered into the cylinder and the convenient quantity of Bakelite poured into the cylinder above the specimen. Next

operations are heating for seven minutes under constant pressure and cooling by a circulation of water for two minutes. Then the hood is removed and the piston lifted. Residual traces of Bakelite must be cleaned after each operation. The method provides a bakelite cylinder easy to handle. Perfect horizontality of the surface to be examined under microscope is achieved by inserting a plastic material between the bakelite cylinder and a slide under manual press.

An alternative method used Koldmount.<sup>54</sup> Two parts of powder are mixed to one part of liquid by volume for not less than 30 seconds and poured over the specimen in the mounting ring placed on a sample holder in glass, stainless steel or Teflon. Twenty minutes at room temperature are required before Koldmount hardens sufficiently. Then it is pushed out of the ring with a brass cylinder, for instance, under a press. Advantage of Koldmount is that it can be dissolved in Methyl Ethyl Ketone so that the sample is recuperated easily without damages for other tests.

2.1.2 A grinding might be necessary before the rough polishing if the material is hard. It can be done, for instance, with a Handimet Grinder, grit 240-320-400-600.<sup>53</sup> Polishing uses generally a series of Emery papers (1/0, 2/0, 3/0, 4/0), size 9" x 13 3/4"<sup>55</sup> or polishing paper rolls 4" x 50 yds.<sup>56</sup>

Soft materials such as gold, silver, copper can be polished directly after cutting. From one paper to the following, orientation of sample must be changed by 90°. Traces or scratches from polishing with the previous paper must have totally been removed. Sample is washed under water and cleaned with ethylic alcohol after each operation. Further polishing can be done with Levigated alumina, 15 $\mu$  or Alpha polishing

alumina N°1,  $5\mu$ , considered as rough polishing - and alpha No. 2 or No. 3,  $0.3$  or  $0.05\mu$ , considered as fine polishing, or diamond paste  $1\mu$  or  $1/4\mu$ , available in disposable tube from reference,<sup>53</sup> using a polishing cloth, canvas or microcloth. These operations are achieved on an automatic turntable such as Polymet,<sup>53</sup> where a sample holder oscillates above a rotary disc - or a Syntron polishing machine<sup>57</sup> which uses a vibratory method.

2.1.3 Etching is necessary for revealing the structure listings of possible etching agents for different materials are very helpful.<sup>58,59</sup> If no agent has been reported for the particular material, one will proceed with some tentative tests under ventilated hood. Consulting chemical properties of the material will help for selecting the proper agents. Conditions of attacks will be determined by experiment. For instance, the Keller's agent (HF 10 ml, HNO<sub>3</sub> 25 ml, HCl 15 ml, H<sub>2</sub>O 50 ml) give good results for the Al-Al<sub>2</sub>Cu eutectic with three successive attacks during 5 seconds separated by washes under flow of water. The sample is washed under water and alcohol and blown dry.

2.1.4 Examination under optical microscope and microphotography. A proper objective is selected, for instance X40. The total magnification is the product of magnifications by the objective and the eyepieces, for instance  $10 \times 40 = 400$ . Some microscopes such as the Ultraphot-II-Zeiss afford illuminations from a tungsten filament or by cesium iodide. The tungsten filament is generally used, except when a more intense illumination is required. A filter, such as a green filter, facilitates observation. In some cases, polarized light allows to enhance contrast. Dark field effects may also be considered. After he has recognized the type

of structure, the operator chooses a representative field and prepares for a photograph. For instance, he puts a Polaroid PN55 film in the film holder and selects an exposure time. After exposure, he has to wait 20 seconds for developing.

### 2.1.5 Typical measurements.

2.1.5.1 Measurements of the interlamellae spacing. The interlamellae spacing is estimated from the photomicrograph. It seems necessary to know the orientation of some direction on the microphotograph with respect to a reference direction of section A, for instance, the intersect line of planes A and B. The use of the stereographic projection allows to determine orientation of the lamellar planes from their traces in two reference surfaces. It is the two surface analysis technique described in references<sup>60,61</sup> and on Fig. 10. The two reference surfaces which are plane A (top section) and B (transversal section) are first plotted on the projection, one surface lying in the plane of projection and forming the basic circle A, the other surface, B, coinciding with the meridian NS, since A and B are orthogonal. On the planes A and B are then located the points  $T_A$  and  $T_B$  which represent the directions of the traces in the two reference surfaces respectively. They lie at angles laid off from the edge NS to correspond with angles  $\psi_a$  and  $\psi_b$  on the specimen. The angles are measured as differences of latitude on the stereographic net. The traces  $T_A$  and  $T_B$  having been plotted, the plane which causes them is drawn by rotating the net so that some single meridian of the net passes through both points. This meridian (c) is the projection of the lamellar plane. Thus it is possible to measure angle  $\theta_4$  between directions  $T_A$  and  $T_B$ . Referring to the method described by Yue,<sup>57</sup>  $\theta_1$ ,  $d_1$  and  $\theta_2$ ,  $d_2$  are

obtained from magnified photomicrographs of sections (A) and (B). Knowing  $\theta_1, \theta_2, \theta_4, d_1, d_2$ , the interlamellar spacing  $\lambda$  can be evaluated from

$$\lambda = d + d' = d_1 \sin \theta + d_2 \sin \theta$$

$$= (d_1 + d_2) \sin \left\{ \cos^{-1} \frac{\overline{SD}^2 + \overline{DC}^2 - \overline{AC}^2}{2 \times \overline{SD} \times \overline{DC}} \right\}$$

where  $\overline{SD} = \overline{SB} \sin \theta$ ,

$$\overline{DC} = \overline{BD} \tan \theta_4 = \overline{SB} \cos \theta_1 \tan \theta_4$$

$$SC = \left( \overline{SB}^2 + \overline{BC}^2 - 2\overline{SB} \times \overline{BC} \cos \theta_2 \right)^{1/2}$$

since  $BC = BD/\cos \theta_4 = SB \cos \theta_1/\cos \theta_4$ , the quantity between the brackets simplifies. ( $SB^2$  is a common factor in numerator and denominator.)

2.1.5.2 Fault density. On a transverse section, it is possible to count the number of positive and negative faults at the traces of mismatch surfaces. These faults are usually developed at the end of an extra lamella. Consult reference (62). Fault density is obtained from the number of faults per unit area. Another characteristic, the distance between mismatch surfaces is measured along the lamellae on the photomicrographs.

2.1.5.3 Banded microstructure. Banding is a solidification phenomenon associated with the liquid solid interface. Often, this transverse defect can be seen with the unaided eye on a polished and etched specimen. It is the result of a change in spacing, discontinuity or irregularity in the lamellar structure.<sup>63</sup> Microstructural evaluations such as no bands, faint banding, or severe banding can be plotted as a function

of growth parameters.

2.1.5.4 Rod-like eutectics. Slightly elongated particles on a transverse section show that the rods are curved.<sup>62</sup> Circular shapes indicate that the rods are perpendicular to the plane of figure. The photomicrographs enable one to calculate the average distance ( $\lambda$ ) between rods and the number of rods per unit cross sectional area. More than 100 measurements of  $\lambda$  are sometimes made on different microphotographs taken from the same sample.

## 2.2 X-ray techniques

2.2.1 Method. Kraft describes a technique for determining orientation relationships and interfacial planes in polyphase alloys and its application to controlled eutectic specimens. The back reflection Laue technique is convenient<sup>64</sup> for large grains. The method is combined with metallographic measurements. However, when the crystallites are small or of varying orientation or if one phase has not a cell with the maximum symmetry, it becomes impractical to interpret the complex overlapping Laue patterns. Indices of the planes in the back-reflection region must be known. For instance, in case of the Al-Al<sub>2</sub>Cu eutectic, Debye-Scherrer photographs are first taken of filings of a heat which is predominantly CuAl<sub>2</sub> ( $\theta$  phase). The lines are indexed. The data show that 424, 622, 514 and 543 and Al 420, 422 reflections are satisfactory. Each of these lines can be easily resolved; all are sufficiently intense. The coordinates of each reflection are plotted on a stereogram using the specimen surface as a reference. One stereogram is made for each phase. Comparisons are made with standard projections of each phase.



2.2.2 Discussion of results. There is one mean orientation for each phase, but within the irradiated area the crystallographic orientation of separate lamellae may vary from the mean by several degrees. Depending on the conditions for solidification, different orientation relationships may be found. For instance:

$$(001) \theta // (001) \text{Al}; [100] \theta // [100] \text{Al} \quad (65)$$

$$(001) \theta // (001) \text{Al}; [100] \theta // [110] \text{Al} \quad (66)$$

Aluminum is expected to grow with [001] normal to the heat flow in castings. Therefore, aluminum platelets would also tend to grow with [001] normal to the heat flow.<sup>67</sup> But the condition of preferred growth in both phases may not be compatible with conditions of minimum interfacial energy. For instance, it was found that Al(112) and CuAl<sub>2</sub> (102) were the low index planes closest to being parallel to the solid liquid interface which was approximately normal to the heat flow. Similar studies were done for the Ni-Ni<sub>3</sub>Ti eutectic.<sup>68</sup> The two surface metallographic technique showed that the lamellae were perpendicular to the polished transverse cross section. Experimental Ni<sub>3</sub>Ti {40 $\bar{4}$ 6} and {42 $\bar{6}$ 1} pole figures were superimposed on standard projections of the Ni<sub>3</sub>Ti lattice. Similarly a nickel {400} pole figure was plotted on the same reference coordinates. Two cubic standard projections twinned on a (111) plane fitted the experimental data.

The local growth direction was considered as perpendicular to the band orientation determined from a photomicrograph. Knoop hardness impressions can be used to take a photomicrograph from the same area as the photomicrograph, and establish the relationship between local growth direction, the ingot axis and the orientation of eutectic phases.

2.3 Electron beam microprobe (X-ray microanalyzer). The electron probe microanalyzer<sup>69</sup> uses an electron beam generated by an electron gun accelerated under several KV and focussed on the specimen by two electron lenses. The electron beam can be restricted to a diameter of less than  $1\mu$  on the specimen. An optical microscope permits the positioning of the area of interest under the beam. Micro-hardness indentations are helpful for this operation. Traces of previous etching have been removed. The composition of a point is determined by comparing the intensities of characteristic X-ray lines of its components with those obtained with a standard of known composition. The method is called the "point by point" counting. Another method, the "line scan" can be performed either by focussing the spectrometers on the spectral lines of the components while the specimen is displaced under the beam or by deflecting the electron beam while the specimen is kept stationary. Beam deflection is limited to  $50\mu$  or less for quantitative measurements. It is possible to obtain images of the composition by the X-ray imaging scanning technique. The instrument is used mainly for identification and quantitative analysis. The range of elements that can be detected corresponds to the range of the spectrometers. They work between 1 and  $10 \overset{\circ}{\text{A}}$ . That is the range covered by the lines of the K, L, M, series of all elements with atomic numbers higher than 11.

The spatial resolution is not limited only by the dimensions of the electron beam. Depth of penetration and lateral spread within the target must be sufficient to excite X-rays. This effect limits the resolution to  $1-2\mu$ . Reducing the beam diameter to less than  $0.5\mu$  does not improve the resolution unless one uses low acceleration voltages and longer wavelengths or specimens thinner than the depth of electron penetration.

As a microanalytical tool, the instrument provides data from a small mass as low as  $10^{-11}$  or  $10^{-10}$  g. without destroying the area. It is not a trace analysis method since the limit of detectable concentration is typically 0.5 to 0.01%, but the absolute amount of an element observed is exceedingly small ( $10^{-16}$  to  $10^{-15}$  g). Three elements are analyzed at the same time. See the microphotographs No. 6 and No. 7, taken with  $\text{CuK}_\alpha$  and  $\text{AlK}_\alpha$  radiation respectively.

Surface of specimen must be conductive or be made conductive to both heat and electricity, in order to limit the rise of temperature which can reach several hundred degrees in case of non-metallic specimens while it is generally less than  $5^\circ\text{C}$  for metals. The electron beam microprobe of Lawrence Berkeley Laboratories has been built by MAC (Palo Alto, Calif.).

#### 2.4 Transmission Electron Microscope (TEM).

2.4.1 Preparation of specimen. For the purpose of determining phase orientation, the thin metal foil technique is compulsory. Preliminary slicing with an abrasive cut-off wheel gives a 0.020" slice. The lower limit is 0.1 mm. Mechanical grinding allows to decrease thickness down to  $100\mu\text{m}$ . Chemical etching is not recommended in the case of polyphase materials since it may be difficult to prevent preferential attack of one phase, unless one wants to remove it selectively. The ion bombardment technique is sometimes used for some difficult cases, but it is very slow (24 hours for removing  $10\mu$  of an aluminum copper alloy).

Electropolishing is the most successful method. Two methods are currently used: the jet polishing technique and the window technique. Spark machined thin discs of diameter 2.3 or 3 mm for compatibility with the sample holders of the Siemens or Hitachi TEM respectively are mounted

perpendicularly to a jet of electrolyte. A photocell detects a beam light when a hole is formed at the center of the disc and stops the operation.

The window technique is described on page 154 of reference 70. The same book contains on page 160 a table which lists electrolyte compositions and polishing conditions for a number of alloys or metals. Referential polishing at specimen edges is avoided by coating with a non-conducting lacquer. A preliminary test provides the voltage-current characteristics. The plateau of the curve corresponds to the constant current suitable for electropolishing.

In some cases, the operation is helped by using low temperatures. For instance, the bath temperature is kept below 20°C by suspending the electrolyte in a container placed over liquid nitrogen. Intermediate relacquing operations take place before final perforation is achieved. Specimens are cut with a sharp steel scalpel from the thin edges near the holes, and placed between two copper grids in the sample holder of the TEM.

2.4.2 Examination of specimen. Thin areas near the hole are less than 1000 Å thick. They are convenient for a selected area diffraction pattern (SAD). Only planes which are approximately normal to the foil surface diffract, because the diffraction angles are very small ( $10^{-2}$  rad.). The diameter of the selected area depends on the voltage. It is about 2μ at 100 KV but is as low as 0.2μ at 1000 KV.

## 2.5 Scanning Electron Microscope (SEM)

The SEM is similar to the TEM.<sup>71</sup> The main differences are the following:

- (a) it gives an image of the surface as a result of excitations induced by the beam, e.g. secondary or reflected electrons,
- (b) the voltage is only 10-25 KV while TEM has 100-1000 KV,
- (c) it accepts bulk sample rather than thin foils,
- (d) SEM uses much lower beam currents. Heating effects are reduced,
- (e) the electron beam scans the sample whereas TEM has a stationary beam.

Brightness and contrast vary with the surface at topographic differences, compositional differences, etc. Specimens must be conductive. SEM is very versatile. It has poorer resolution in reflection than TEM, but different types of information from the sample can be displayed on separate CRTS. SAD analysis is possible although on a coarser scale than is possible by TEM. SEM can also be used as a microanalyzer.

#### 2.6. Summary of Methods for Characterization of Oriented Eutectics

Eight samples taken from the literature can be consulted in Table III for comparison.

Table III

No.	Alloy	Polishing and Etching for Optical Microscope	Electron Microscope
1	Al-Cu-Mg	<ul style="list-style-type: none"> <li>-sections taken 4 cm from the end first solidified</li> <li>-mechanically polished to Linde A, then electropolished in a solution of 5% sulfuric acid and 1 1/4 % hydrofluoric acid in methanol at 30 V for about 1 sec.</li> <li>-immersion stain etch in a solution 1% nitric acid, 1% hydrofluoric acid and 1% hydrochloric acid in water</li> </ul>	<ul style="list-style-type: none"> <li>-thin foils prepared by slicing 15 to 20 mil blanks on an abrasive saw and mechanically thinning them to approx. 2 mils</li> <li>-these blanks were electropolished in a solution of three parts methanol and one part nitric acid at 35 to 40 V and -40°C</li> <li>-examination in a Philips EM300</li> </ul>
2	Ni-Al-Cr		<ul style="list-style-type: none"> <li>-samples etched in a 3% oxalic acid at 5 V to remove the Ni Al matrix phase</li> <li>-observation in a SEM</li> <li>-TEM+SAD of transverse sections</li> </ul>
3	Co-Cr-C	<ul style="list-style-type: none"> <li>-etching: heated solution of 20% potassium ferricyanide</li> </ul>	<ul style="list-style-type: none"> <li>-TEM (Hitachi HU-11, under 100 kV), specimens prepared by electrolytically thinning a transverse slice of material in a solution of 85 parts acetic acid and 15 parts perchloric acid maintained at 10°C</li> <li>-SAD</li> </ul>

Table III. continued

No.	X-Ray Methods	Other Tests	References
1		-An ARL Electron microprobe was used to obtain X-ray images of the phases in polished surfaces	-Met. Trans., <u>3</u> , 533 (1972)
2	-Laue back reflection patterns for determining orientation of individual grains -Lattice parameters of the two phases were determined by X-ray diffraction both on bulk samples and on powders from the ingots		-Met. Trans., <u>1</u> , 2799 (October 1970)
3		-Composition of the alloy determined by chemical analysis -Composition of the eutectic phases obtained by point count analysis using a Philips AMR/3 electron probe analyzer	-Met. Trans., <u>1</u> , 2799 (October 1970)

Table III. continued

No.	Alloy	Polishing and Etching for Optical Microscope	Electron Microscope
4	(Fe-Cr)-Nb	<ul style="list-style-type: none"> <li>-electroetched in a saturated Oxalic acid solution for 20 sec at 6 V</li> <li>-volume fraction of the minor phase estimated in a "Quantimet" quantitative television microscope on etched samples</li> </ul>	<ul style="list-style-type: none"> <li>-matrix phase (iron chromium solid solution) preferentially removed by a 5 min electroetch in saturated oxalic acid solution at 20°C, 6 V potential and a current density of 0.85 to 0.90 amp per sq cm</li> <li>-examination in a "Stereoscan" SEM</li> </ul>
5	Mg-Mg <sub>2</sub> -Ni	<ul style="list-style-type: none"> <li>-specimens were mounted, wet ground through 600 grit LiC abrasive, and final polishing at a moderate low speed on a microcloth lap covered with a thick slurry of 1<math>\mu</math> Al<sub>2</sub>O<sub>3</sub> in a very dilute solution of NH<sub>4</sub>OH (one drop of NH<sub>4</sub>OH per 500 ml of deionized water)</li> <li>-cleaned with cotton while submerged in the NH<sub>4</sub>OH solution quickly rinsed in hot tap water and blown dry</li> <li>-magnesium matrix was prone to galvanic attack and no further preparation was necessary</li> </ul>	



Table III. continued

No.	X-Ray Methods	Other Tests	References
4	<p>-structure and lattice parameters determined by standard X-ray diffraction techniques</p>	<p>-tensile specimens prepared by conventional machining and grinding methods (L=1.4 cm, D=0.5 cm)            -stained at various temperatures between 20° and 1000°C in a TF-K model Instron machine            -SEM microfractographs</p>	<p>-Met. Trans.,  <u>3</u>, 551            (February 1972)</p>
5	<p>-a transmission pole figure technique was used to determine the orientations of the two phases with respect to one another and the solidification axis            -metallographic trace analysis provided the additional information needed to specify the five degrees of freedom of the Mg-Mg<sub>2</sub> Ni interface            -determination of the indices of a twinning plane using the fact that the basal pole in the twinned material is a mirror image in the twinning plane of the basal pole in the untwinned material</p>	<p>-tensile specimens, L=1.00 in., D=0.15 in.            -compression specimens cylinders D=0.230 in., H=0.500 in.            -strain rate: 0.01 per minute on a Instron testing machine</p>	<p>-Met. Trans.,  <u>3</u>, 611            (March 1972)</p>

Table III. continued

No.	Al <sub>3</sub> Ni-Al	-mechanical polishing down to the 1 diamond pad stage followed by an electropolish in 80/20 methanol/perchloric acid solution at 0°C and 20 to 30 V (Ref. b)	-a slice 0.05 cm thick was cut and mechanically thinned to 0.005 cm. The blank was electrolytically thinned in a solution of three parts methanol and one part nitric acid at 203 K and 40 V. Examination in a Philips EM-300 at 100 kV TEM+SAD gave orientations between the phases. Interfacial planes were determined by trace analyses of at least two zones for both the rod and matrix (Ref. a) -thin films prepared by spark machining thin discs (0.03 to 0.04 in. thick) from longitudinal and lateral sections and electrolytically thinning them via a jet polishing technique in a 80/20 mixture of ethanol/perchloric acid at 40 V and 20°C (jet nozzle cathodes and disc clamps were of aluminum) (Ref. b)
7	Sn-Zn	-repeatedly polished on an alumine pad and etched in hot dilute (2%) nitric acid	-discs electrolytically thinned in a 70/20/10 methanol/perchloric acid/butylcellosolve at 25 V and 20°C via a jet polishing technique (jet nozzles cathodes and disc clamps were of stainless steel)
8	Cu-Cu <sub>2</sub> S	-specimens were mechanically polished through to 1/4 diamond paste and etched in a solution of 20% acid ferric chloride in alcohol for approx. 20 sec -Interrod specimens were measured on transverse sections of specimens. On each sample 100 individual measurements of λ were made on micrographs taken at a magnification of ×750.	-specimens were mechanically polished through to 4μ diamond paste and then deeply etched in acid ferric chloride for 6 min. This dissolved the copper to a depth of 2 to 3μ and eliminated any of the Cu <sub>2</sub> S particles sectioned by the initial polishing. Examination in a Stereoscan SEM. -Orientation of Cu <sub>2</sub> S was determined by electron diffraction of particles on extraction carbon replicas.

000003900000

Table III continued

No.		
6	Laue back reflection technique with a finely focused X-ray source	a) Met. Trans. <u>4</u> , 707 (1973) b) Trans. AIME <u>245</u> , 2435 (1969)
7	-the orientation of the matrix phase (copper) was determined using the X-ray back reflection Laue method on both longitudinal and transverse sections Method did not work with Cu <sub>2</sub> S which gave insufficient spots.	Trans. AIME, <u>245</u> , 2435 (1969)  Met. Trans. <u>2</u> , 2681 (1971)
	- the proportion of Cu <sub>2</sub> S was measured on both transverse and longitudinal sections, at a magnification of ×1000 by means of a "Quantimet" image analyzing computer.	

## 3. APPENDIX

Recent Bibliography of Phases Orientation  
in Directionally Solidified Eutectics

From: Metallurgical Transactions & Transactions AIME.

- Crystallography and Morphology of As-Grown and Coarsened Al-Al<sub>3</sub>Ni Directionally Solidified Eutectics. G. Garmon, C. G. Rhodes and R. A. Spurling, March 1973.
- Stability of the Directionally Solidified Eutectics - NiAlCr and NiAlMo. J. W. Walter and H. E. Cline, Vol. 4, Jan. 1973, 33.
- Structure and Mechanical Properties of the Directionally Solidified Al-Cu-Mg eutectic, Vol. 3, Feb. 1972, 533-544.
- Mg-Mg<sub>2</sub>Ni Eutectic Composite  
K. H. Eckelmeyer and R. H. Hertzberger, Vol. 3, March 1972, 609-616.
- Structures, Faults and the Rod-Plate Transition in Eutectics  
H. E. Cline, J. L. Walter, E. Lifshin and R. R. Russell, 189-194, 1971.
- The Morphology and Thermal Stability of the Cu-Cu<sub>2</sub>S Eutectic System, p. 2681-2689. S. Marich and D. Jaffrey, Vol. 2, Sept. 1971, 2681-2689.
- Discussion of the "Lamellar to Fibrous Transition" and Orientation Relationships in the Sn-Zn and Al-Al<sub>3</sub>Ni Eutectic Systems. M. J. Salkind, Vol. 1, June 1970, 1786.
- Unidirectional Solidification of Co-Cr-C Monovariant Eutectic Alloys  
E. R. Thompson and F. D. Lemkey, Volume 1, Oct. 1970, 2799-2806.
- The Effect of Alloy Additions on the Rod Plate Transition in the Eutectic NiAl-Cr.  
Harvey E. Cline and John L. Walter, Vol. 1, Oct. 1970, 2907-2917.

- The Lamellar to Fibrous Transition and Orientation Relationships in Sn-Zn and Al-Al<sub>3</sub>Ni Eutectic Systems, D. Jaffrey and G. A. Chadwick, Vol. 245, p. 2435-2440.
- Microstructures and Crystallography of the Ni-Ni<sub>3</sub>Ti Eutectic Alloy, K. D. Sheffler, R. W. Kraft and R. W. Hertzberg. Vol. 245, p. 227-231.
- Crystallography of Equilibrium Phase Interfaces in Al-CuAl<sub>2</sub> Eutectic Alloys, R. W. Kraft, Vol. 224, Feb. 1962-65-75.
- Technique for Determining Orientation Relationships and Interfacial Planes in Polyphase Alloys, R. W. Kraft, Trans. AIME, 1961, Vol. 221, 304, 704-710.

From: ACTA METALLURGICA

- Fine Structure Investigation in Lead Rich Phase of PbSn Lamellar Eutectic, M. G. Blanchin, A. Guinier, C. Petitpas et G. Sauvage, Vol. 20, Nov. 1972, 1251.
- Structure and Properties of Aluminum Silicon Alloys, H. A. Steen and A. Hellawell, Vol. 20, March 1972, 363.
- High Speed Solidification of Several Eutectic Alloys, J. D. Livingston, H. E. Cline, E. F. Koch and R. R. Russell, Vol. 18, April 1970, 399.

From: JOURNAL OF APPLIED PHYSICS

- Electron Microscopic Study of Thin Films of the Aluminum-Copper Eutectic Prepared by a Melting Method, Nobora Takaheshi, Vol. 31, No. 7, July 1960.

From: JOURNAL OF CRYSTAL GROWTH

- Effects of Growth Rate on the Morphology of Monovariant Eutectics:  
MnSb - (Sb, Si) and MnSb - (Sb-Sn), M. Durand-Charre and F. Durand  
13/14 (1972) 747-750.
- Cellular Morphologies in Rapidly Solidified Al-Al<sub>2</sub>Cu and Al-Al<sub>3</sub>Ni  
Eutectic Alloys, W. H. S. Lawson and H. W. Kerr and M. H. Lewis  
12 (1972) 209-216.
- Structure of Bi-Ag Eutectic Alloy - T. G. Digges, Jr. and R. N. Tauber  
8 (1971) 132-134.
- Transmission Electron Microscopy of Eutectic Alloys in Al-Zn and Cd-Zn,  
6 (1969) 107-108, D. D. Double and A. Hellawell.

#### Acknowledgments

This work was done under the auspices of the U. S. Atomic Energy Commission through the Inorganic Materials Research Division of the Lawrence Berkeley Laboratory.

REFERENCES

Part I.

1. K. A. Jackson, Liquid Metals and Solidification, p. 174, ASM, Cleveland, Ohio (1958).
2. K. A. Jackson, Growth and Perfection of Crystals, R. H. Doremus, D. Turnbull, and W. Roberts, Eds., p. 319, John Wiley, New York (1958).
3. J. D. Hunt and K. A. Jackson, Tr. AIME, Vol. 236, June 1966, 843.
4. H. W. Kerr and W. C. Winegard, Eutectic Solidification in Crystal Growth, Proceedings of an International Conference on Crystal Growth, Boston, 20-24 June 1966, edited by H. Stefan Peiser, The Journal of Physics and Chemistry of Solids, supplement No. 1., 1967, p. 179.
5. M. Hansen and K. Anderko, "Constitution of Binary Alloys," McGraw-Hill Book Company, New York, 1958.
6. R. Hultgren, et al., Selected Values of Thermodynamic Properties of Metals and Alloys, John Wiley, New York, (1963).
7. D. J. S. Cooksey, D. Munson, M. P. Wilkinson and A. Hellawell, Phil. Mag. 10, 745 (1964).
8. M. D. Rinaldi, R. M. Sharp and M. C. Flemings, "Growth of Ternary Composite from the Melt: Part I, Metallurgical Transactions, Vol. 3, Dec. 1972, p. 3133, Part II, p. 3139.
9. H. W. Terr, A. Plumtree and W. C. Winegard, J. Inst. Metal, 1964-65, Vol. 93, p. 63.
10. D. J. S. Cooksey and A. Hellawell, J. Inst. Metals, 1967, Vol. 95, p. 183.

11. Ha-Quac-BaO: Thesis, Universite' de Grenoble, 1970.
12. G. Garmong, Metal. Trans., 1971, Vol. 2, p. 2025.
13. H. Bibring, J. P. Trottier, M. Rabinovitch, and G. Seibal, Mem. Sci. Rev. Met., 1971, Vol. LXVII, No. 1, p. 23.
14. E. R. Thompson and F. D. Lemkey, Met. Trans., 1970, Vol. 1, p. 2799.
15. J. L. Walter and H. E. Cline, Met. Trans., 1970, Vol. 1, p. 1221.
16. E. R. Thompson and F. D. Lemkey, Trans. ASM, 1969, Vol. 62, p. 140.
17. S. E. R Hiscocks, J. Mater. Sci., 1969, Vol. 4, p. 773.
18. D. J. S. Cooksey, M. G. Day and A. Hellawell, The Control of Eutectic Microstructures in Crystal Growth, (4) p. 151.
19. W. A. Tiller, Liquid Metals and Solidification, p. 276, ASM, Cleveland (1958).
20. K. A. Jackson, "Progress in Materials Science," edited by G. A. Chadwick, 12 (2)(1963).
21. G. A. Chadwick, "Progress in Materials Science," 12 (2) (1963).
22. H. W. Kerr, J. A. Bell and W. C. Winegard, J. Australian Inst. Metals, 10, 64 (1965).
23. Bruce Chalmers, Principles of Solidification, p. 207, John Wiley.
24. A. S. Yue, Trans. AIME, Vol. 212, 1958, p. 320.
25. W. A. Tiller, K. A. Jackson, J. W. Rutter and B. Chalmers, Acta. Met., 1953, Vol. 1, p. 428.
26. H. Weart and D. Mack, Tr. AIME, Vol. 212, 1958, p. 320.
27. H. E. Cline, Trans TMS-AIME, 1968, Vol. 242, p. 1613.
28. G. Garmong, Met. Trans., Vol. 3, March 1972, p. 741.
29. J. P. Chilton and W. C. Winegard, J. Inst. Met., 224, 1176 (1961).
30. G. A. Chadwick, J. Inst. Met., 91, 169 (1963); 92, 18, (1963).



31. R. W. Kraft, D. L. Albright, Tr. AIME, Vol. 221, Feb. 1961, p. 95.
32. W. G. Pfann, Zone Melting, John Wiley, 1958, p. 153.
33. as (23), p. 302.
34. Techniques of Metals Research, R. F. Bunshah, Editor, Part I -  
Temperature Measurement and Control, D. L. McElroy and W. Fulkerson,  
p. 244.
35. as (34), p. 177.
36. Gilman, The Art and Science of Growing Crystals, John Wiley, New  
York, p. 317.
37. as (36) p. 343.
38. as (4), R. J. Brigham, G. R. Purdy and J. S. Kirkaldy, p. 161.
39. R. A. Laudise, The Growth of Single Crystals, Prentice-Hall, Inc.,  
p. 203.
40. Robert Bakish, Ed., Introduction to Electron Beam Technology, Wiley,  
New York, 1962, pp. 168, 184.
41. as (4), p. 75, Walter Class, Harvey R. Nesor, and G. T. Murray.
42. as (4), p. 171, F. D. Lemkey and M. J. Salkind.
43. as (39), p. 165.
44. T. S. Noggle, Rev. Sci. Instr. 24, 184 (1953).
45. as (39), p. 163.
46. as (4), p. 201, H. P. Utech, W. S. Brower and J. G. Early.
47. as (4), p. 645, J. R. Carruthers and W. C. Winegard.
48. as (4), p. 651., H. P. Utech and M. C. Flemings.
49. as (39), p. 166-167.
50. K. H. Eckelmayer and R. W. Hertzberger, Metal Trans. AIME, Mar. 1972,  
p. 609.

## Part II.

51. Servomet, available from Metals Research Ltd., Cambridge, England.
52. Hardman Inc., Belleville, N. J. 07109.
53. Buehler Ltd., Greenwood Street, Evanston, Ill. 60204
  - bakelite powder, by quantities of 5 pounds.
  - Handimet grinder.
  - diamond paste 1 or 1/4  $\mu$ .
  - canvas microcloth.
  - polymet rotary discs.
54. Vernon-Benschhoff Co., 413 No. Pearl St., Albany, New York -  
Koldmount powder.
55. Behr-Manning Co., Troy, New York (a subdivision of Norton Co.)  
packages of 100 emery papers, 9" x 13 3/4", 1/0, 2/0, 3/0, 4/0.
56. 3M Co., St. Paul, Minn. 55101, SYNTRON, Homer City, Penn.
57. SYNTRON, Homer City, Penn.
58. George L. Kehl, The Principles of Metallographic Laboratory Practice,  
McGraw Hill Book Company, 1943.
59. ASM (Metals Engineering Institute) Metallographic Appendix, by  
R. S. Crouse.
60. Charles S. Barrett, Structures of Metals, McGraw-Hill Book, 1952.
61. Techniques of Metals Research, Volume II, Part I, p. 259, R. E. Reed  
Hill - Editor: R. F. Bunshah, 1963, Interscience Publishers.
62. A. S. Yue, Trans. AIME, Vol. 224, Oct. 1962, 1010.
63. R. W. Kraft, D. L. Albright, Trans. AIME, 221, 1961, 95.

64. R. W. Kraft, Trans. AIME, Vol. 221, p. 704,
65. E. C. Ellwood and K. Q. Bagley, The Structure of Eutectics, J. Inst. Metals, 1949, Vol. 76, pp. 631-42.
66. N. Takahasi, J. Appl. Phys., 1960, Vol. 31, No. 7, pp. 1287-90.
67. as 60, p. 511.
68. K. D. Sheffler, R. W. Kraft, and R. W. Hertzberger, Trans. AIME, Vol. 245, Feb. 1969, pp.227-231.
69. K. F. J. Heinrich, National Bureau of Standards, Washington, D.C.
70. G. Thomas, Transmission Electron Microscopy of Metals, John Wiley & Sons, Inc., p. 150.
71. G. Thomas, Modern Metallographic Techniques, UCRL-19697.

## FIGURES

- Fig. 1. Surface energy vs volume fraction for rods and lamellae eutectics.
- Fig. 2. Diagrammatic representation of eutectic growth profiles.
- Fig. 3. Hypothetic phase diagram impurity-eutectic.
- Fig. 4. Schematic representation of regions of different structural stability for hypothetical systems. Arbitrary scale of temperature gradient and freezing rate.
- Fig. 5. Three basic experimental methods of growth with an horizontal furnace.
- Fig. 6-1. Vertical furnace.
- Fig. 6-2. Bridgmann-Stockbarger growth-method of lowering crucible.
- Fig. 6-3. Movable resistance wound radiation furnace.
- Fig. 7. Electron bombardment melting.
- Fig. 8. Examples of temperature gradients.
- Fig. 9. Typical horizontal furnace - distribution of fluids - temperature control - mechanical transmission.
- Fig. 10. Two surface analysis techniques.

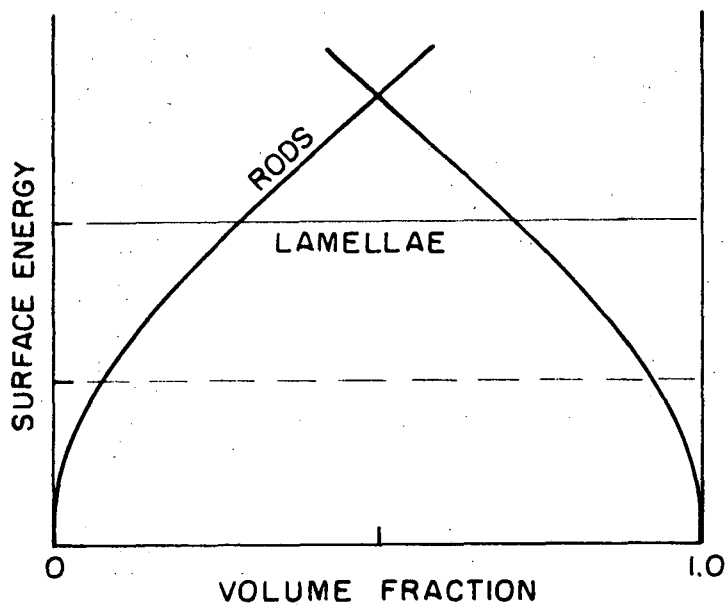


FIGURE 1

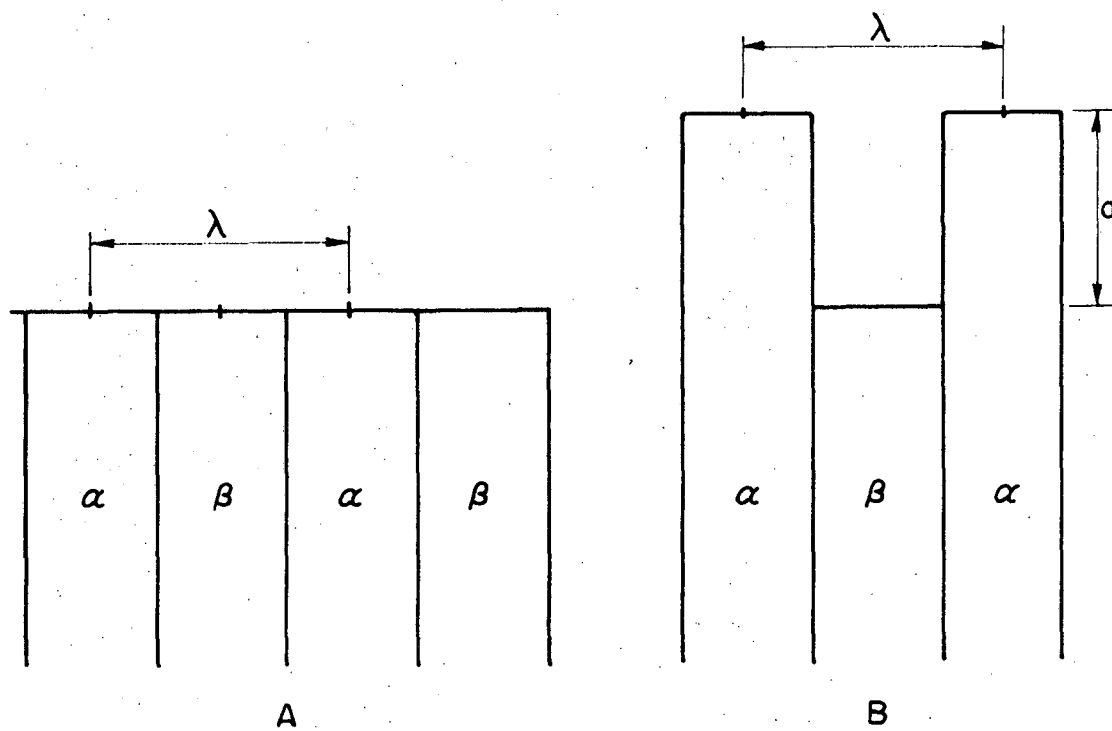


FIGURE 2

ABL 736-6271

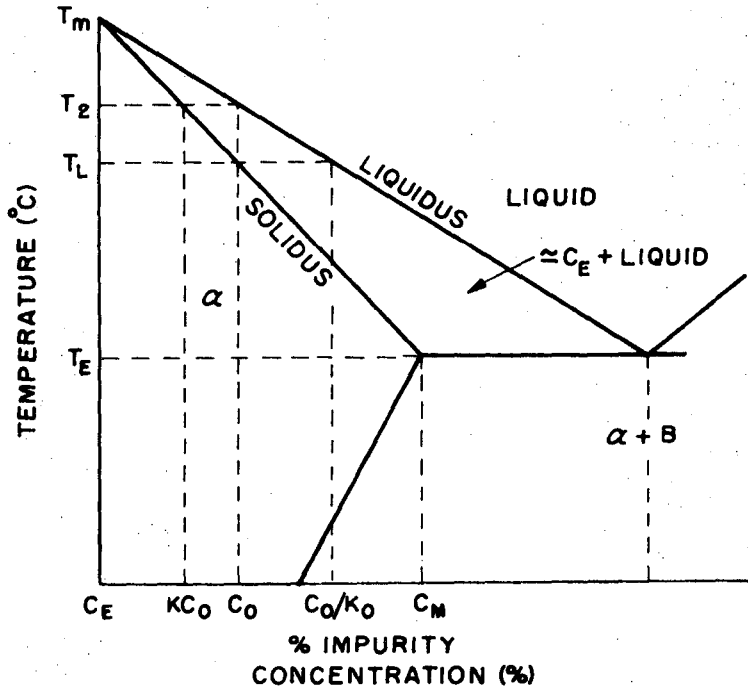


FIGURE 3

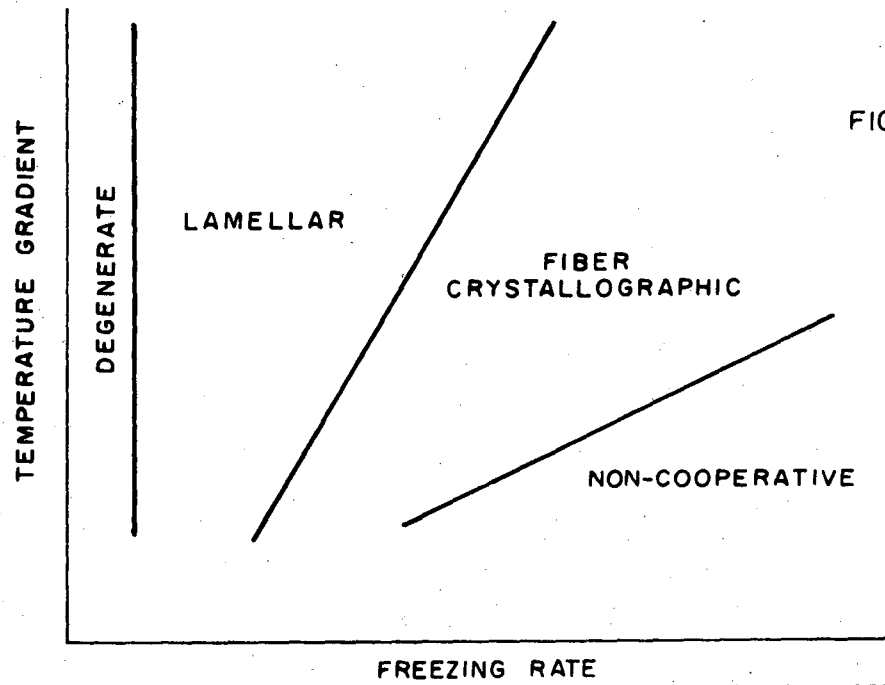
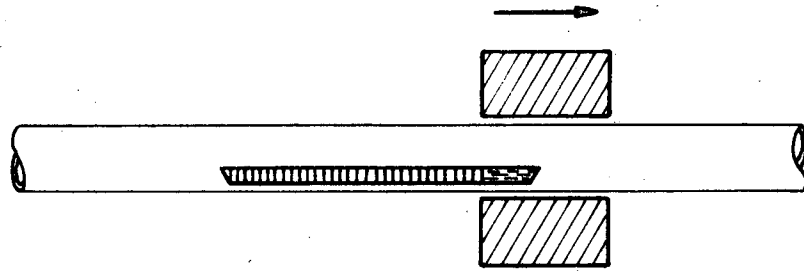
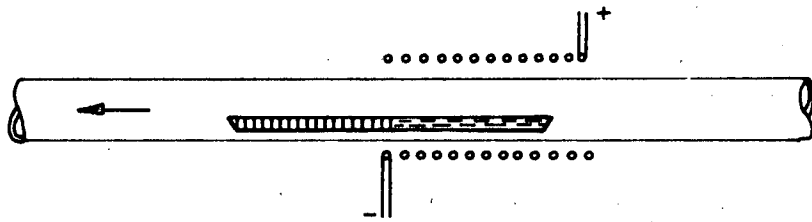


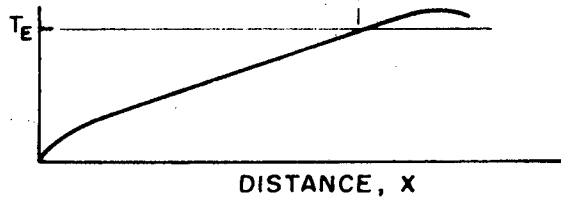
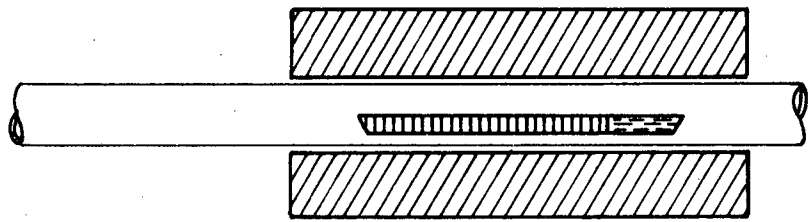
FIGURE 4



FIRST METHOD



SECOND METHOD

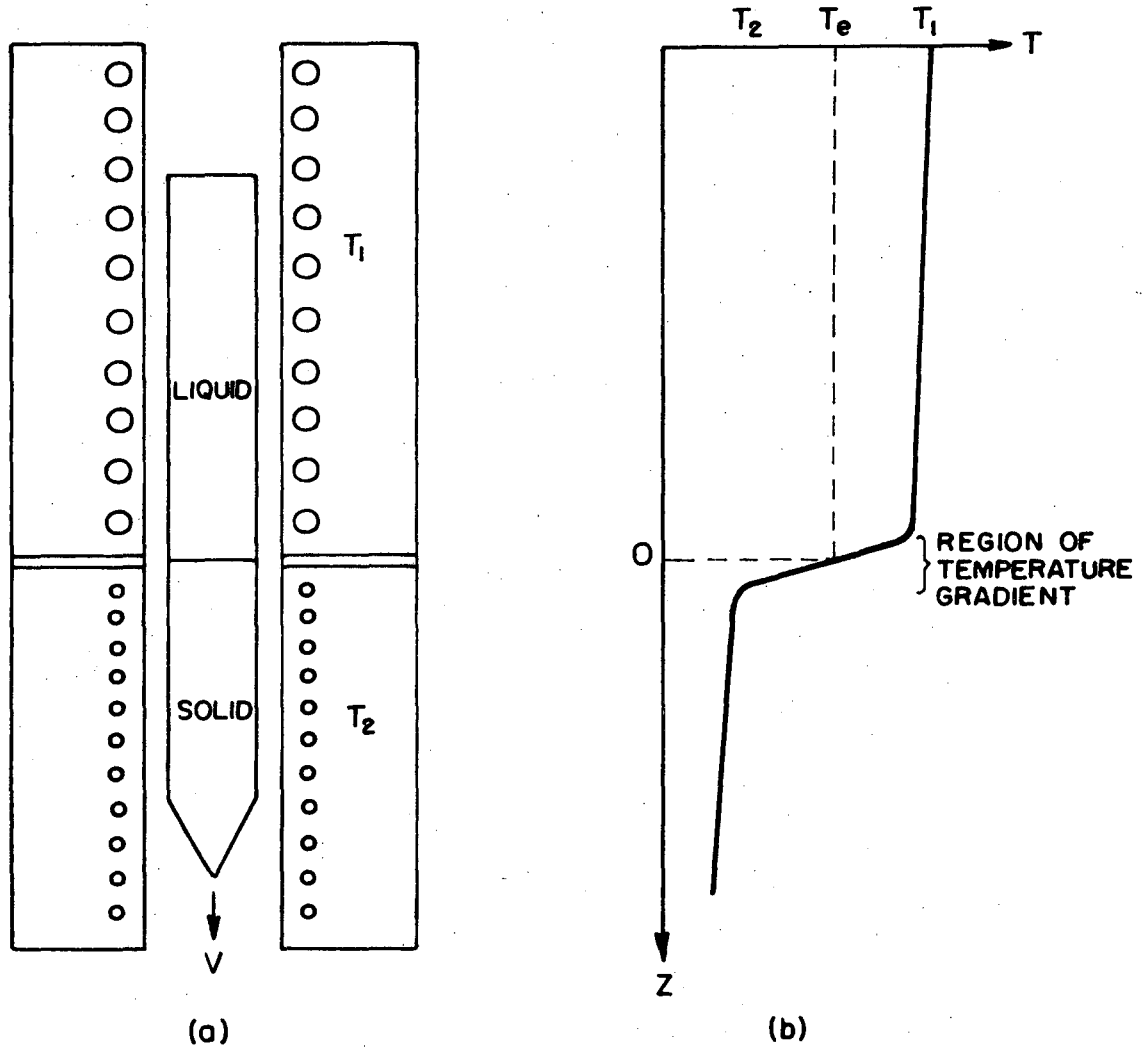


THIRD METHOD

XBI. 736-6273

FIGURE 5

FIGURE 6-1  
Vertical Furnace



XBL 736-6274

- (a) Two stage furnace composed of two thermal reservoirs between which a crucible containing the alloy is passed at constant velocity,  $V$ .
- (b) Temperature distribution along the axis of motion. Reproduced from "Eutectic-Type" Phase Transformation by Lee F. Donaghey, March 1969, p. 10.



FIGURE 6-2  
Bridgman-Stockbarger Growth Method of Lowering Crucible

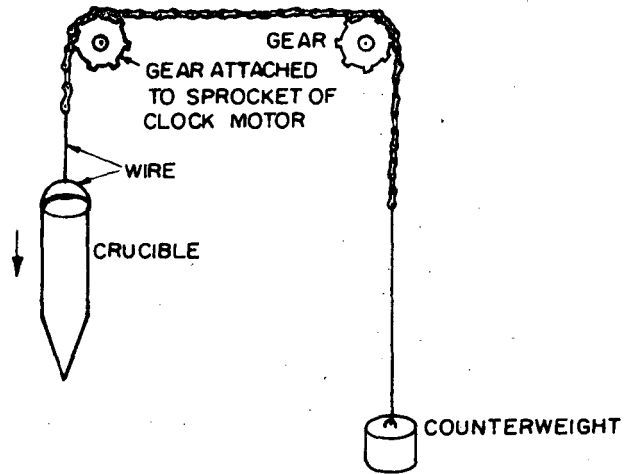
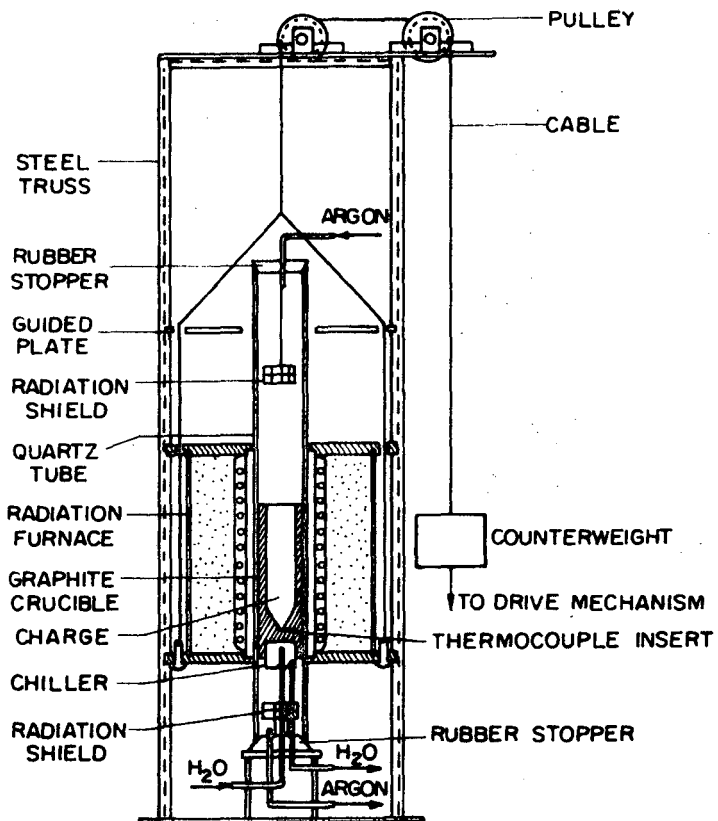


FIGURE 6-3

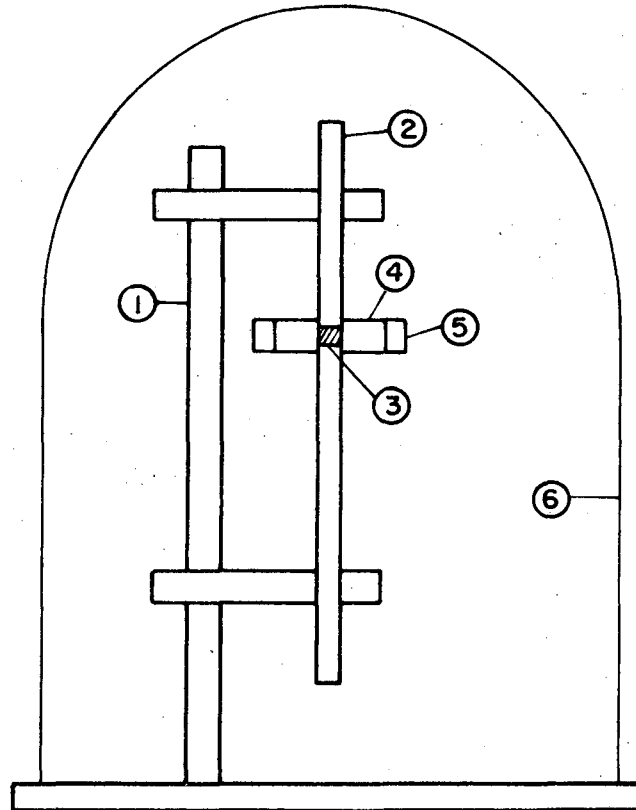


XBL 736-6275

Moveable Resistance-Wound Radiation Furnace

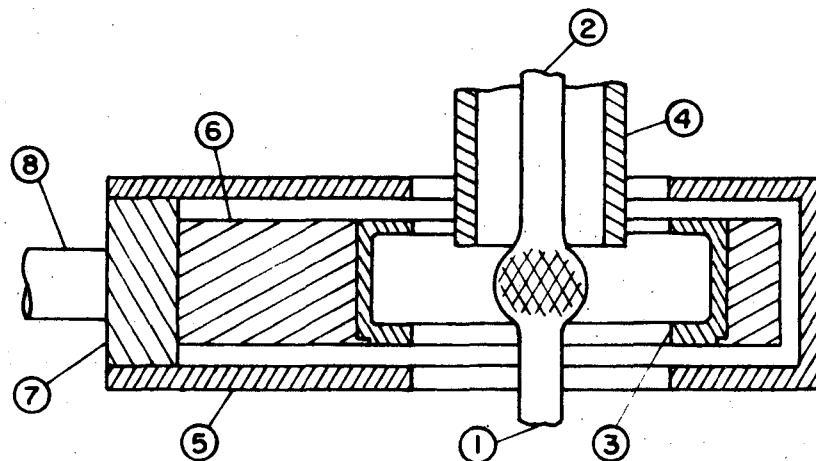
FIGURE 7

Electron Beam Melting Filament Emitter



- 1. Sample Holder
- 2. Sample
- 3. Melt
- 4. Ring Filament  
Electron Emitter
- 5. Reflector Plates
- 6. Bell Jar

Hollow Cathode Technique



XBL 736-6276

- 1. Feed Rod, 2. Oriented Material, 3. Hollow Cathode, 4. Beam Divergence  
Shield, 5. Cathode Shield, 6. Water Cooled Cathode Holder, 7. Boron  
Nitaide Insucator, 8. Water and Power Input

FIGURE 8

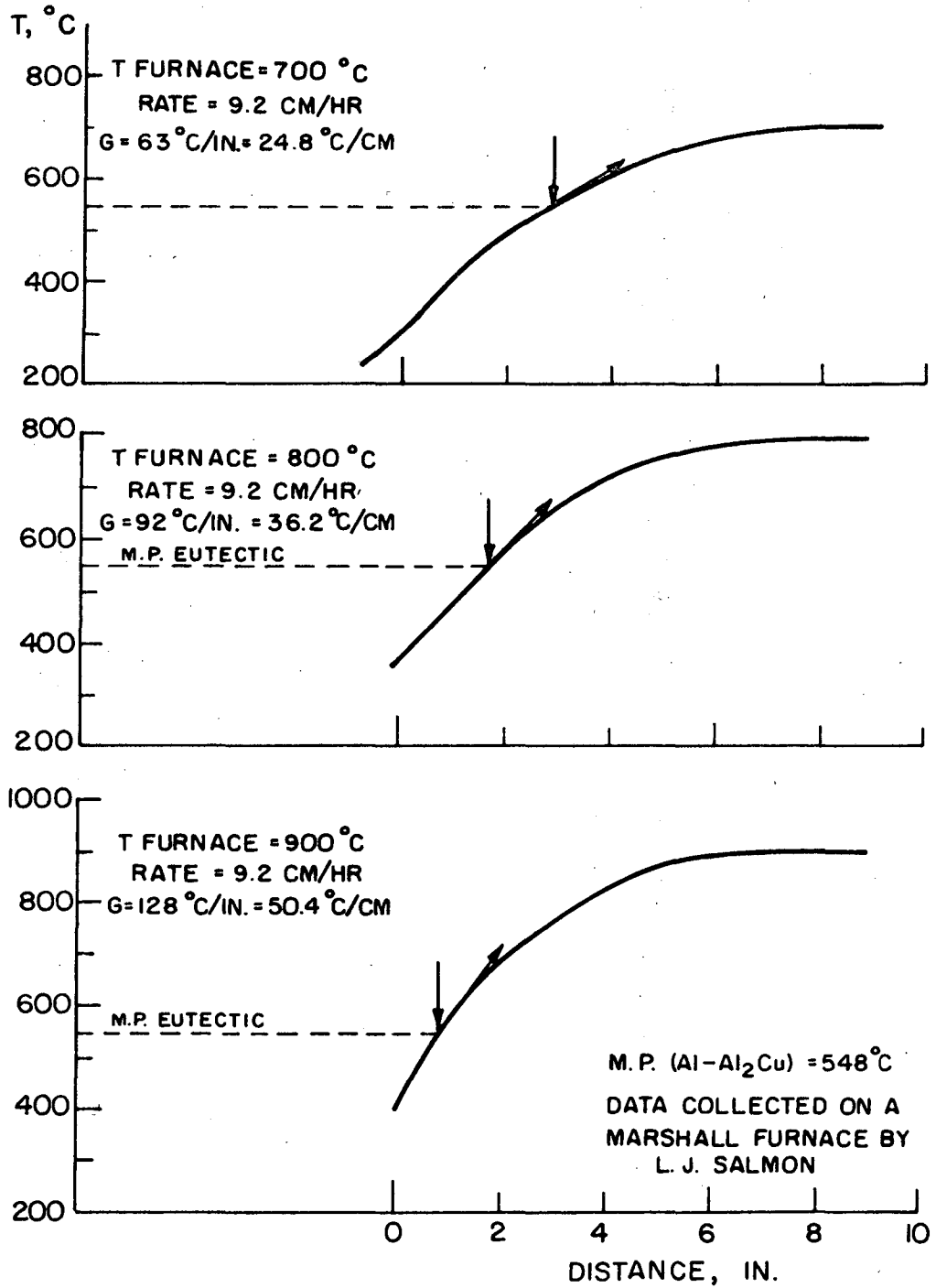
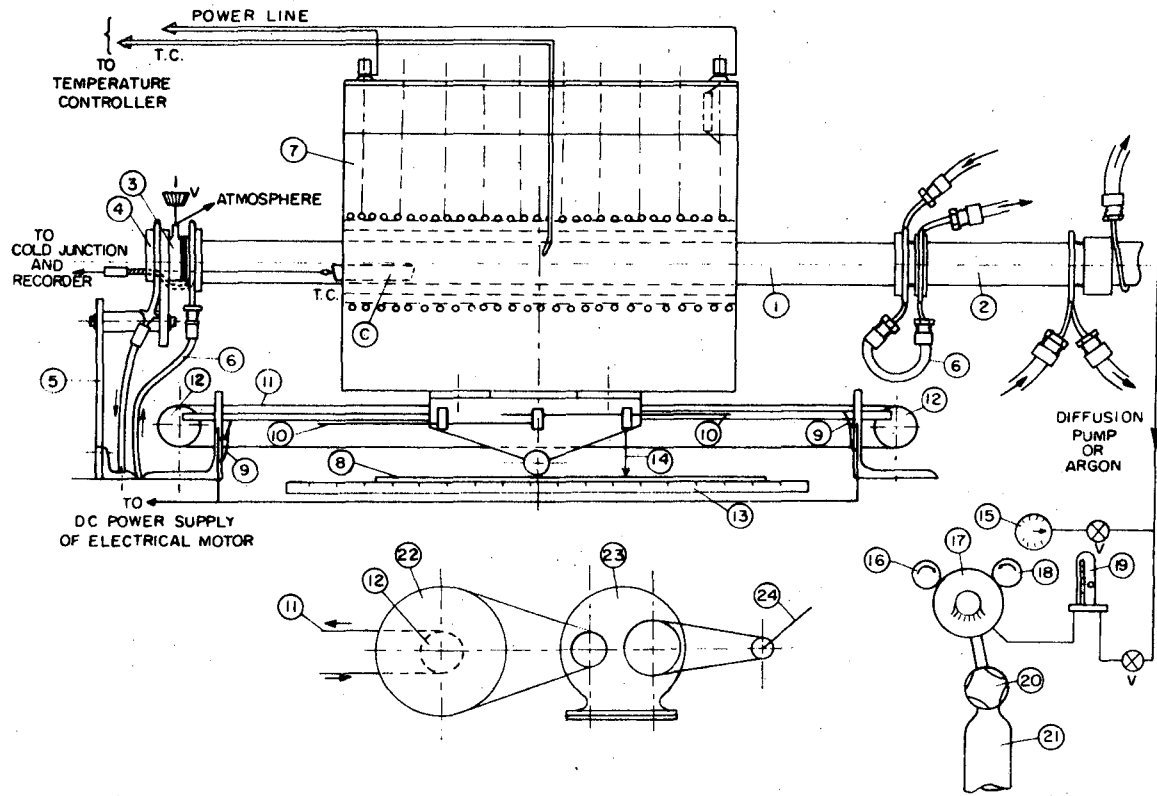


FIGURE 9



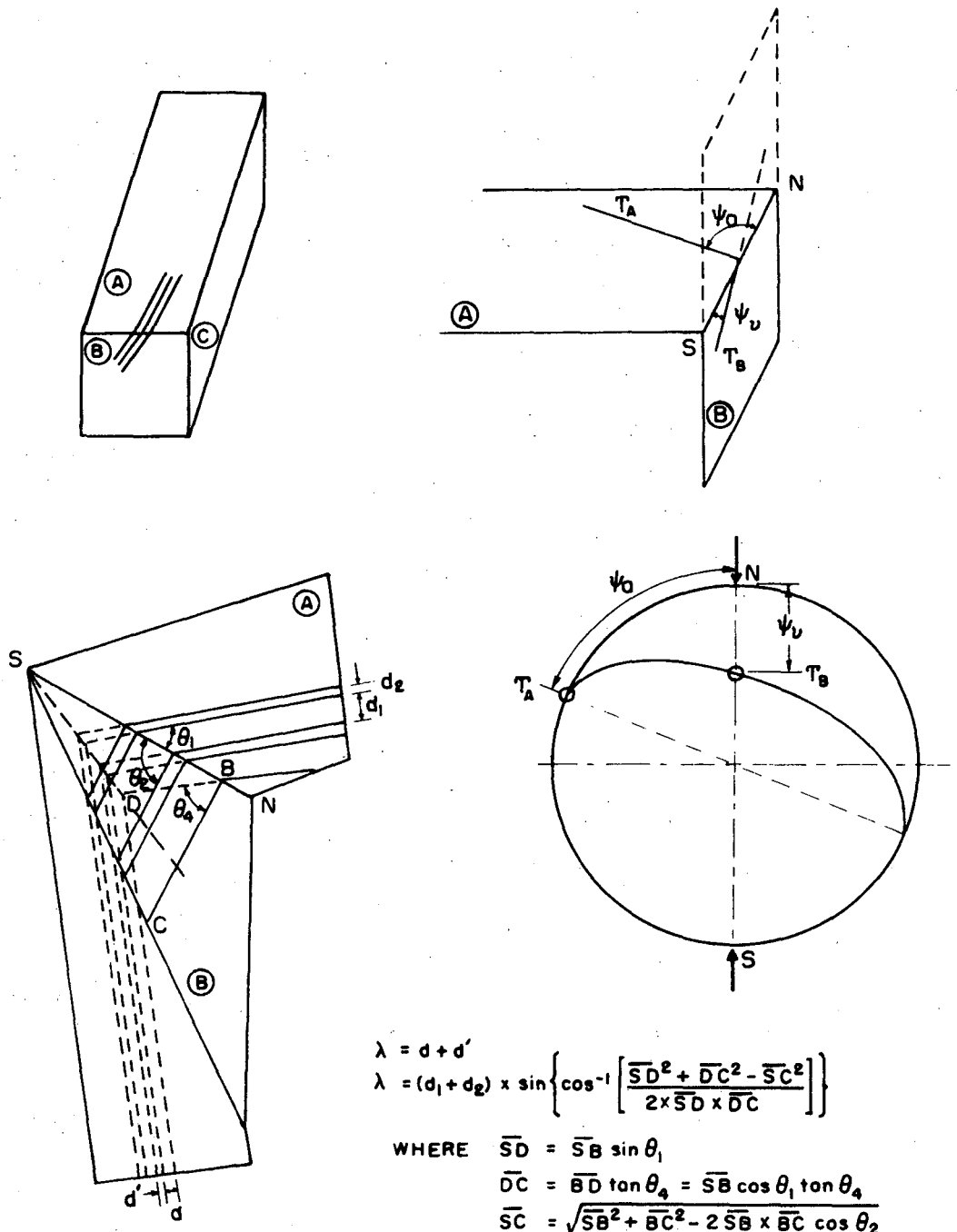
XBL 736-6278

Figure 9

INDEX

- 1 - Quartz tube with crucible (C).
- 2 - Copper tube.
- 3 - Support of quartz tube (copper).
- 4 - Copper end disc with O-seal ring and thermocouple passage.
- 5 - Aluminum support.
- 6 - Water colling system.
- 7 - Moving furnace, front and end face: asbestos, laberal side:  
aluminum sheet, Marshall furnace, Max. AMP = 14.7.
- 8 - Track
- 9 - Switch-end of course.
- 10 - Adjustable rods.
- 11 - Stainless steel wire for mechanical transmission.
- 12 - Drums (D=21).
- 13 - Scale
- 14 - Pointer
- 15 - Indicator of pressure on line.
- 16 - Indicator of pressure after regulator.
- 17 - Regulator
- 18 - Indicator of pressure on tank.
- 19 - Flowmeter
- 20 - Valve of argon tank.
- 21 - Argon tank.
- 22 - Pulley  $P_1$ .
- 23 - Bear box.
- 24 - Electrical motor shaft.

FIGURE 10



$$\lambda = d + d'$$

$$\lambda = (d_1 + d_2) \times \sin \left\{ \cos^{-1} \left[ \frac{\overline{SD}^2 + \overline{DC}^2 - \overline{SC}^2}{2 \times \overline{SD} \times \overline{DC}} \right] \right\}$$

WHERE  $\overline{SD} = \overline{SB} \sin \theta_1$   
 $\overline{DC} = \overline{BD} \tan \theta_4 = \overline{SB} \cos \theta_1 \tan \theta_4$   
 $\overline{SC} = \sqrt{\overline{SB}^2 + \overline{BC}^2 - 2 \overline{SB} \times \overline{BC} \cos \theta_2}$

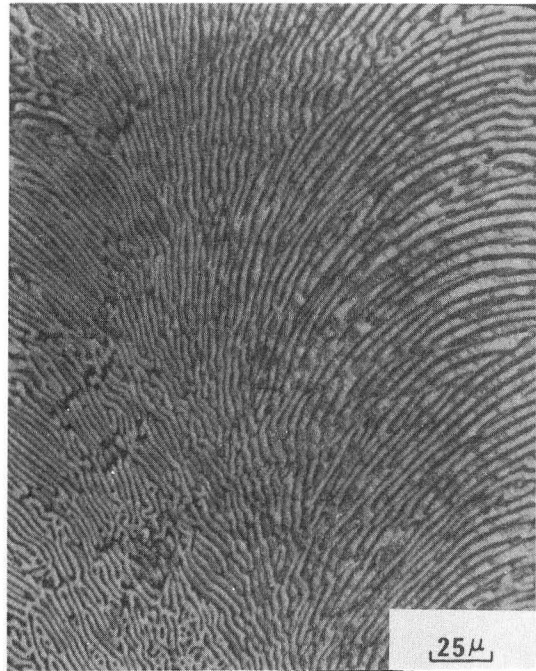
$\theta_1, \theta_2, \theta_4, d_1, d_2$  ARE MEASURABLE

MICROPHOTOGRAPHS

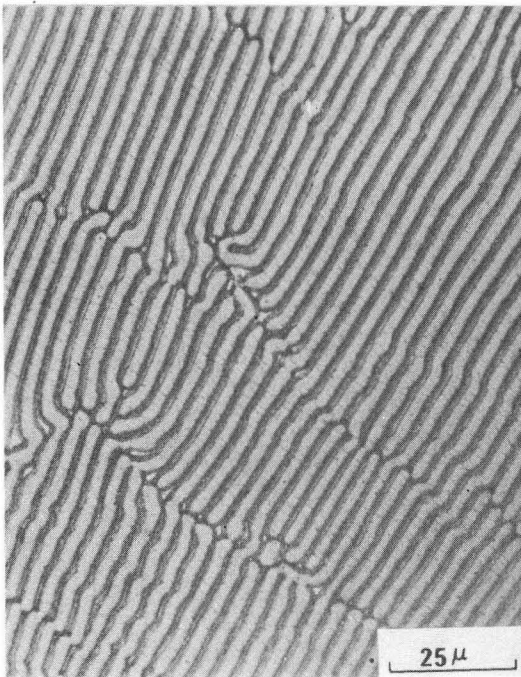
- 1 - Al-Al<sub>2</sub>Cu Eutectic-non-directionally frozen- (X 400)
- 2 - Al-Al<sub>2</sub>Cu Eutectic-directionally frozen (horizontal furnace)  
R = 9.18 cm/h, G = 50 °C/cm, top section, cellular  
substructure, X 400
- 3 - Al-Al<sub>2</sub>Cu Eutectic-directionally frozen (horizontal furnace),  
R = 0.918 cm/h, G = 46°C/cm, transverse section, X 800
- 4 - Al-Al<sub>2</sub>Cu Eutectic-directionally frozen (horizontal furnace),  
R = 0.918 cm/h, G = 46°C/cm, top section, X 400
- 5 - Al-Al<sub>2</sub>Cu Eutectic, R = 0.143 cm/h, G = 57°C/cm  
Back scattered Electrons Image, taken with the Electron Beam  
Microprobe, X 1000
- 6 - Grown as (5), CuK<sub>α</sub> X-ray image taken with the Electron Beam  
Microprobe
- 7 - Same view as (6), AlK<sub>α</sub> X-ray image taken with the Electron Beam  
Microprobe, X 1000



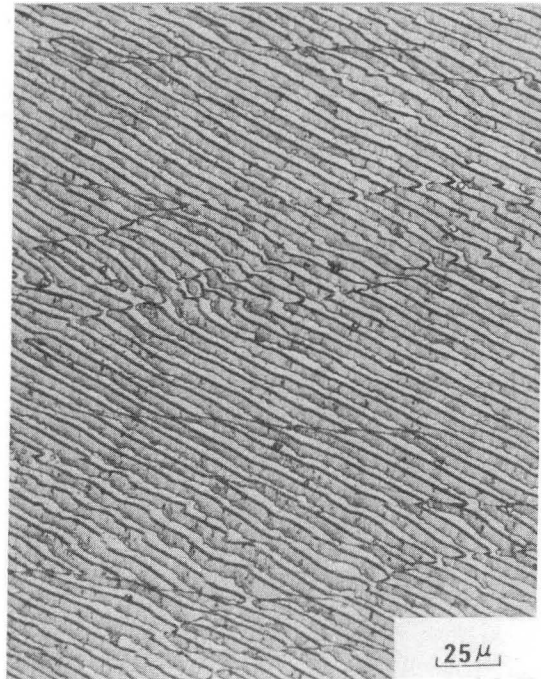
1



2



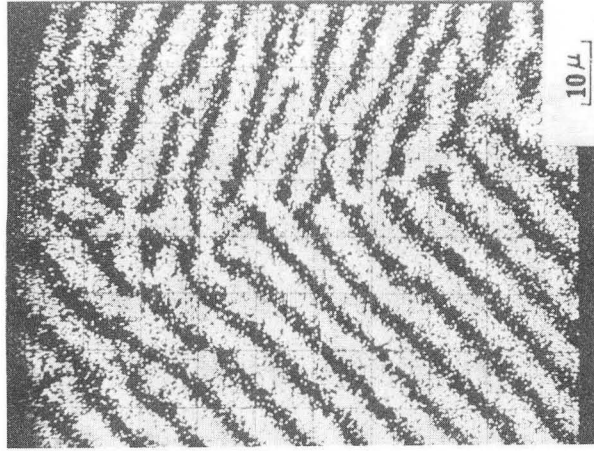
3



4

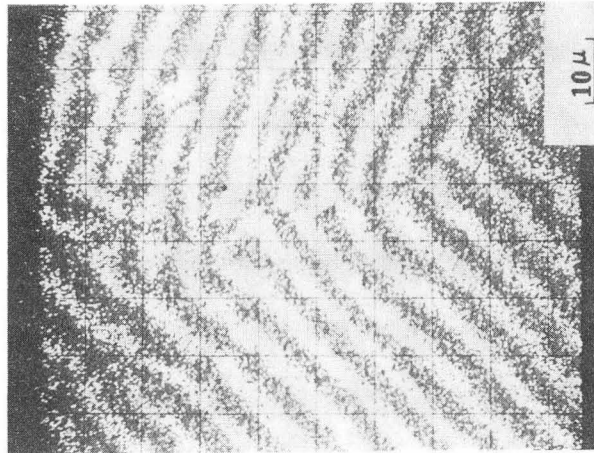
XBB 736-3531



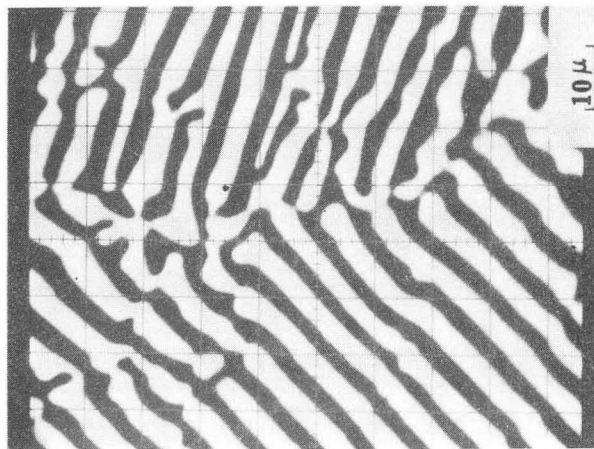


XBB 736-3532

7



6



5

LEGAL NOTICE

*This report was prepared as an account of work sponsored by the United States Government. Neither the United States nor the United States Atomic Energy Commission, nor any of their employees, nor any of their contractors, subcontractors, or their employees, makes any warranty, express or implied, or assumes any legal liability or responsibility for the accuracy, completeness or usefulness of any information, apparatus, product or process disclosed, or represents that its use would not infringe privately owned rights.*

TECHNICAL INFORMATION DIVISION  
LAWRENCE BERKELEY LABORATORY  
UNIVERSITY OF CALIFORNIA  
BERKELEY, CALIFORNIA 94720